Dynamical systems in biology
BIO-341

Fall semester 2024

Julian Shillcock, SSV, julian.shillcock@epfl.ch
Felix Naef, SSV, felix.naef@epfl.ch

Contents

1. Population dynamics in one dimension (1D)

1.1 Dynamical systems (DS): formalism and bases

Dynamical systems theory designates the set of mathematical and numerical methods that allows to study problems involving variables that change as a function of time (or of another equivalent parameter). Non-linear systems are particularly interesting because they generate complex dynamics that are often difficult to predict.

Examples:

- Celestial mechanics

- Chemical kinetics applied to genetic networks

- Protein molecular dynamics

- Population dynamics, ecosystems

- Activation of cellular signaling pathways (e.g. in developmental biology or cancer)

- Circadian clock

Circadian oscillators (molecular clocks with a period of about 24 hours) are often modeled by systems of ordinary differential equations which capture the chemical kinetics of messenger RNAs and proteins involved in this genetic network (Figure 1.1).
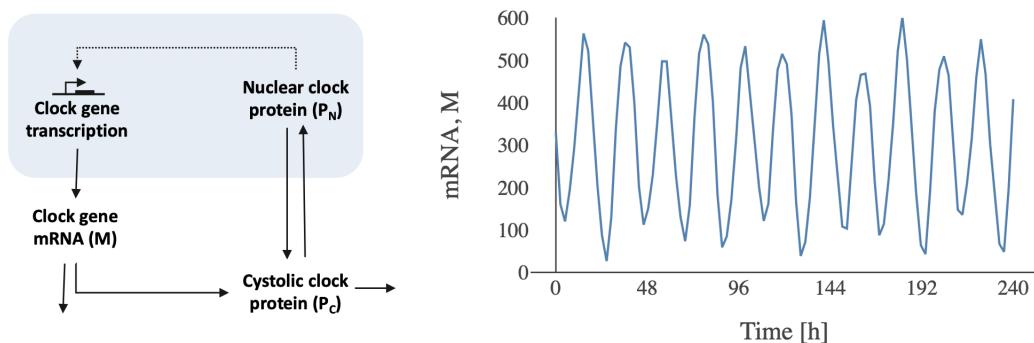
Fig. 1.1. Left: Simplified intra-cellular diagram of a circadian oscillator (here the Gonze-Goldbeter model). Right: Result of a numerical simulation of the differential equations that represent the network on the left. This is a simulation with noise.

There are two main types of dynamical systems::

- Differential equations (*continuous* time):

$$\frac{d\mathbf{x}}{dt} = F(\mathbf{x}(t)), \quad \mathbf{x} \in \mathbb{R}^n \text{ for a function of time } \mathbf{x}(t).$$

   Example: $\frac{dx}{dt} = ax$, (exponential growth)

- Discrete dynamical systems (*discrete* time):

$$x_{n+1} = F(x_n)$$

   Example: $x_{n+1} = \cos(2\pi x_n)$.

We will focus mainly on continuous-time systems which are generally more used to model chemical or biological phenomena.

1.1.1 Definitions

Definition 1.1.1 The generic form of an autonomous system of ordinary differential equations (ODE) is written (here in vector notation):

$$\frac{d\mathbf{x}}{dt} = F(\mathbf{x(t)}) \quad , \quad \mathbf{x} \in \mathbb{R}^{\mathbf{n}} \tag{1.1}$$

Where:

- $\mathbf{x}(t) = (x_1(t), x_2(t), \ldots, x_n(t))$ is a trajectory in a space of dimension n,

- $F(\mathbf{x}) = (f_1(x), f_2(x), \ldots, f_n(x))$ is a vector function that defines the dynamical system.

- n characterizes the dimension of the system

The system is said to be linear if $F(x)$ is a linear function in x. We will often be interested in the case where F is nonlinear in x.

Notations

- $\dot{x} \equiv \frac{dx}{dt}$

The component form is written:

$$\begin{cases} \dot{x}_1 = \frac{dx_1}{dt} &= f_1(x_1, x_2, \ldots, x_n) \\ \dot{x}_2 = \frac{dx_2}{dt} &= f_2(x_1, x_2, \ldots, x_n) \\ \quad \vdots \\ \dot{x}_n = \frac{dx_n}{dt} &= f_n(x_1, x_2, \ldots, x_n) \end{cases}$$

Examples of nonlinear dynamical systems

- Population dynamics for a population $N(t)$

$$\frac{dN}{dt} = F(N) = rN(1 - \frac{N}{K})$$, where $F(N)$ is a second degree polynomial

- Chemical kinetics for the formation of a dimer $A + B \rightleftharpoons C$.

  According to the *law of mass action*:

$$\begin{cases} \dot{A} &= -k_1 AB + k_{-1} C \\ \dot{B} &= -k_1 AB + k_{-1} C \\ \dot{C} &= k_1 AB - k_{-1} C \end{cases}$$

  Here we have written the concentrations without the square brackets: $A \equiv [A]$. k_1 and k_{-1} are the reaction rates (forward and backward).

- An equation with higher order derivatives can be reduced to a system with first derivatives, by adding variables. For example,

$$\frac{d^2 x}{dt^2} = x^2 \implies \begin{cases} \dot{x} = y = f_1(x,y) \\ \dot{y} = x^2 = f_2(x,y) \end{cases} ,$$

  where $y = \dot{x}$.

1.2   Solutions of dynamical systems

> **Definition 1.2.1** The solutions $\mathbf{x}(t)$ of equation 1.1 are called *trajectories* or *orbits*. They depend on a vector of initial conditions $\mathbf{x}_0 = \mathbf{x}(t = 0)$ of dimension n.

In rare cases they can be calculated explicitly, in most cases they are calculated numerically, or their qualitative behavior is established using geometric methods (qualitative analysis). This course mainly studies the latter approach.

1.2.1   Analytical methods (not often applicable)

Separation of variables (for 1-dimensional systems). This method applies to equations that can be written in the form

$$A(t)dt + B(x)dx = 0 \ .$$

We can then integrate $\int_0^t A(t)dt = -\int_{x_0}^x B(x)dx$. The key is i) to solve the integrals, then ii) to derive an explicit form for $x(t)$.

1.2.2   Numerical methods

-   Principle: Taylor expansion

-   Euler method: it is the simplest method that will be sufficient for this course.

$$\mathbf{x}(t+dt) = \mathbf{x}(t) + \frac{d\mathbf{x}}{dt}(t)\,dt + \mathcal{O}(dt^2) = \mathbf{x}(t) + F(\mathbf{x}(t))dt + \mathcal{O}(dt^2)$$

    and therefore $\mathbf{x}(t) + F(\mathbf{x(t)})dt$ is an approximation for the trajectory at time $\mathbf{x}(t+dt)$. The error at each time step is of the order of dt^2 and therefore the global error for a trajectory $n = T/dt$ is of order of dt. The idea is therefore to take a short increment dt.

-   There are other, more accurate techniques, in particular the Runge Kutta method of order 4.

1.2.3   Geometric method and qualitative analysis

This method, which employs an approach that enables understanding of the qualitative behavior of solutions, is particularly suitable for 1D and 2D problems. This approach is useful because it is simple, general, and works well with numerical simulations. This method will mostly be developed in this course, alongside numerical simulations.

1.3   Qualitative analysis in 1-dimension (1D)

We will approach the subject with the simplest case, i.e. in $1D$. The two-dimensional case will be treated in chapters 3 and 4. In $1D$, the principle is as follows: The aim is to represent "the derivative $\dot{x}$ (speed) in function of the position".

Example: $\dot{x} = \sin(x)$ (the damped pendulum)
The following typical questions will then be asked:

- For a given initial condition, will the solution $x(t)$ converge to an equilibrium point? Will it oscillate? Will it grow to infinity?

- How do solutions depend on model parameters?

How do we proceed?
Solve the problem exactly? It is difficult and rarely possible.
In this particular case, the problem can be solved by separation of variables:

$$\int_{x_0}^{x} \frac{dx}{\sin(x)} = \int_{0}^{t} dt = t = -\ln\left|\frac{\csc x_0 + \cot x_0}{\csc x + \cot x}\right| \text{ with } \csc(x) = \frac{1}{\sin(x)}.$$

This is an implicit form because $t = t(x)$ and not $x = x(t)$. Inverting the equation is perhaps possible but surely tedious. The implicit form is difficult to interpret and it is therefore difficult to answer the questions asked above.
On the other hand, the following geometric analysis is clear and simple.

1.3.1   Stepwise qualitative analysis

1. Draw the function $F(x)$ in function of x. This is referred to as Graph 1.

2. Mark the intersections with the horizontal. The intersections correspond to the *fixed points*, given by $F(x) = 0$. "These are points that do not move with time". See 1.3.2 for a precise definition.

3. Indicate with arrows the direction of the speed between the fixed points. Determine the stability of the fixed points. See 1.3.2.

4. Sketch a few representative trajectories $x(t)$. Draw x in function of t. The graph of the trajectories as a function of time are referred to as Graph 2. Note that it is often important to know the slope of the trajectories at the initial point, i.e., at time zero. This is easily obtained from the dynamical equation by substituting in the initial value x_0, and evaluating the derivative dx/dt.
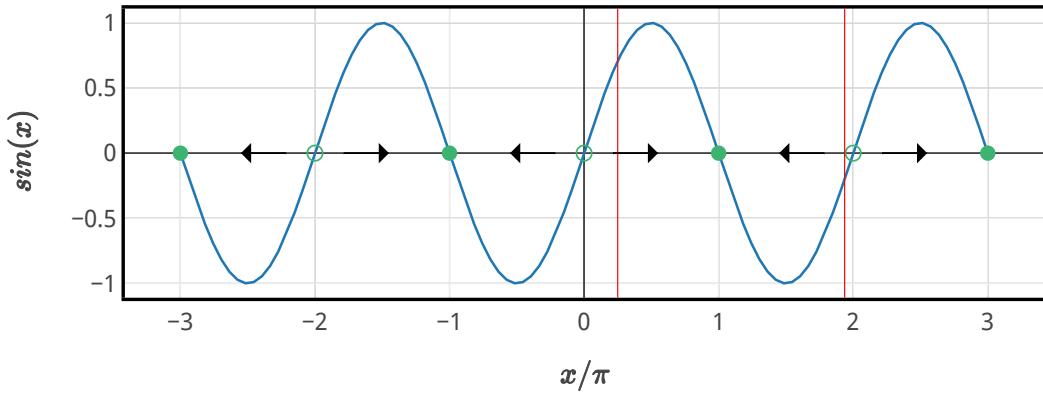
Fig. 1.2. Representation of $\dot{x} = F(x)$ as a function of x for $\dot{x} = \sin(x)$. The filled points (respectively empty) represent points which attract (respectively repel) the trajectories: these are the stable (unstable) fixed points also called attractors (repellants or sources). The arrows indicate the direction of the trajectories.

The solutions $x(t)$ move on the horizontal axis with speed $\dot{x} = F(x)$ as shown in Figure 1.2 . With this representation, we can immediately deduce the trajectories for an initial population $x_0 = x(t = 0)$. Draw some of these trajectories in Figure 1.3 for:

1. $x_0 = \pi/4$

2. $x_0 = 2\pi - \varepsilon$ (for example $\varepsilon = 0.1$)

1.3.2 Fixed points (FPs) and their stability

Definition 1.3.1 The *fixed points* are all points x^* such that

$$F(x^*) = 0.$$

It is where the function F(x) intersects with the horizontal axis.

Examples:

- $F(x) = 1$, no fixed points

- $F(x) = x^2 - 1$, two fixed points $x^* = -1, 1$

There are **three types** of fixed points in 1D:

- **Stable:** $F(x) > 0$ for $x < x^*$ and $F(x) < 0$ for $x > x^*$.

- **Unstable:** $F(x) < 0$ for $x < x^*$ and $F(x) > 0$ for $x > x^*$.
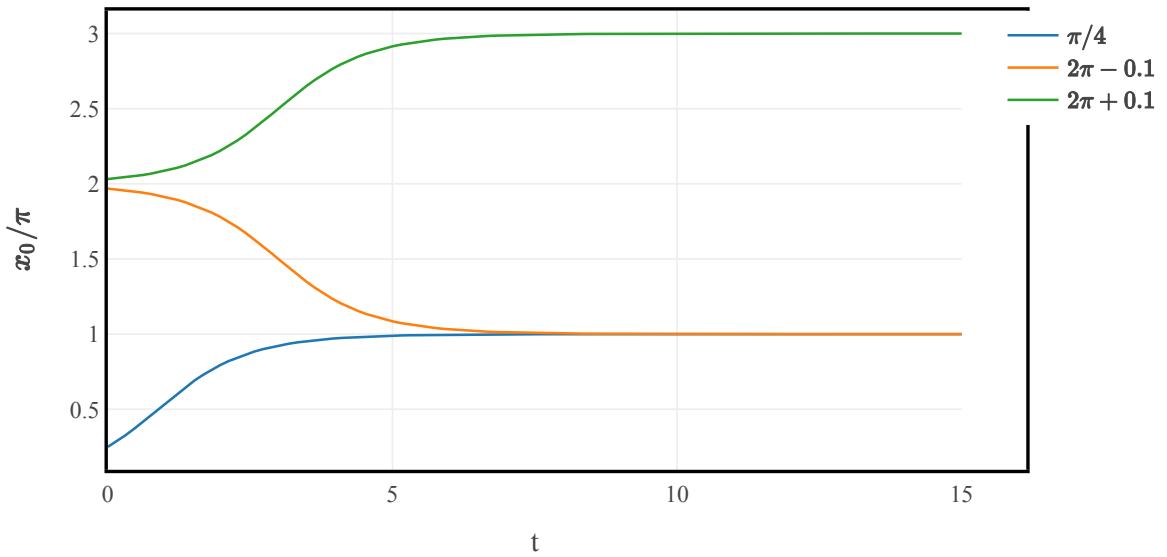
Fig. 1.3. Representation of trajectories for $\dot{x} = \sin(x)$. The initial conditions are $x_0 = \pi/4$ and $x_0 = 2\pi \pm \varepsilon$.

- **Semi-stable:** $F(x) > 0$ for $x < x^*$ and $F(x) > 0$ for $x > x^*$ or $F(x) < 0$ for $x < x^*$ and $F(x) < 0$ for $x > x^*$.
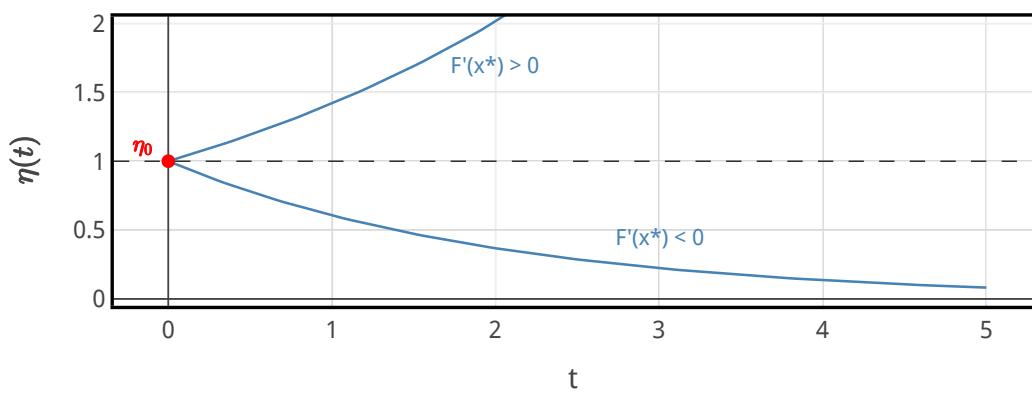
Fig. 1.4. Solutions of the equation for $\eta(t)$ for an initial condition η_0.

Linear stability of FPs in $1D$

Here we will formalize the notion of stability of FPs. To study the stability of a fixed point x^*, we linearize the dynamics around x^*. In other words, we study the dynamic behavior *in the neighbourhood* of x^*.

To do this, we define the following change of variable:

$$\eta = x - x^*$$
$$\dot{\eta} = \dot{x} = F(x - x^* + x^*) = F(\eta + x^*) \simeq F(x^*) + \eta F'(x^*),$$

with $F'(x^*) = \frac{dF}{dx}$, which gives a differential equation for η with the solution $\eta(t) = \eta_0 \, e^{t F'(x^*)}$.

Corollary: The stability to linear order is determined by $F'(x^*)$. $F'(x^*)$ defines an inverse time scale that determines the time it takes to move away from (or approach) the fixed point x^*.

- If $F'(x^*) < 0$ we speak of a linearly stable fixed point.

- If $F'(x^*) > 0$ we speak of a linearly unstable fixed point

- The linear stability is undetermined if $F'(x^*) = 0$. If $F'(x^*) = 0$ it is necessary to study the stability by developing to order η^2, but then we no longer speak of linear stability.

1.4   Growth models for given species

A limitation of equation $\dot{N} = (n-m)N + a$ as a realistic model of a population is that the population explodes to infinity if the birth rate is greater than the death rate: no limitation of resources is taken into account. Also note that $N = 0$ is not a fixed point.

A class of generic population growth models $N(t)$ can be written as:

$$\dot{N} = R(N)N$$

where the function $R(N)$ is the relative growth rate. By definition $N = 0$ is always a fixed point.

Examples:

- Exponential growth: $R(N) = \text{const.}$

- Logistic growth: $R(N) = r(1 - \frac{N}{K})$

- Allee effect (see exercises)

1.4.1   Logistic equation analysis (LE)

<u>Motivation:</u> The exponential growth model with $R(N) = \text{const.}$ ignores the resource limitations in the environment. Thus, it is more realistic to build models where the relative growth rate decreases with population size.

Let us begin by studying the simplest case: that where the relative rate decreases linearly with N: $R(N) = r(1 - N/K)$.

The logistic equation is therefore written as:

$$\dot{N} = R(N)N = rN(1 - \frac{N}{K}), \qquad \text{polynomial of degree 2 in } N,$$

with r and K as positive constants.
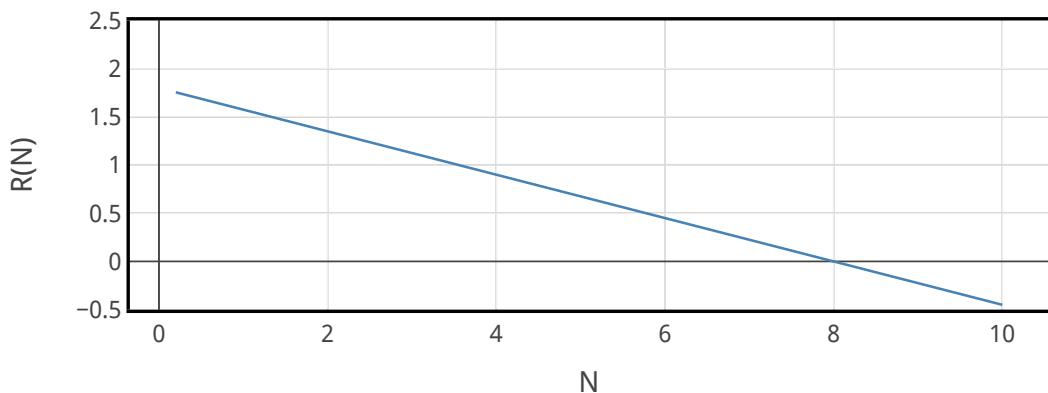
Fig. 1.5. Relative growth rate for the logistic model. The capacity of the environment is K and the ordinate r is the short-term growth rate. Here we have chosen $r = 1.8$ and $K = 8$.

Interpretation of parameters:

- r is the *relative growth rate* when the population is very small ($N \to 0$).

- K is the size of the population for which the growth rate vanishes: it is a fixed point of the dynamics. K is also called the environment *capacity*.

By separation of the variables (to be checked), one can find an analytical solution for an initial population N_0:

$$
\begin{aligned}
N(t) &= N_0 \frac{e^{rt}}{1 + \frac{N_0}{K}(e^{rt} - 1)} \implies \\
N(t) &\simeq N_0\, e^{rt} \qquad \text{for } N_0 \ll K \quad \text{et} \quad t \to 0 \\
N(t) &\simeq K\big(1 - e^{-rt}(\frac{K}{N_0} - 1)\big) \quad \text{for } t \to \infty
\end{aligned}
\tag{1.2}
$$

Exercise: Check the calculation and understand the limits. The different limits are shown in Fig. 1.8

1.4.2 Qualitative analysis

We are only interested in populations $N \geq 0$.

Points 1-3 (Cf. 1.3.1): $F(N)$ vs. N. Cf. Figure 1.6.
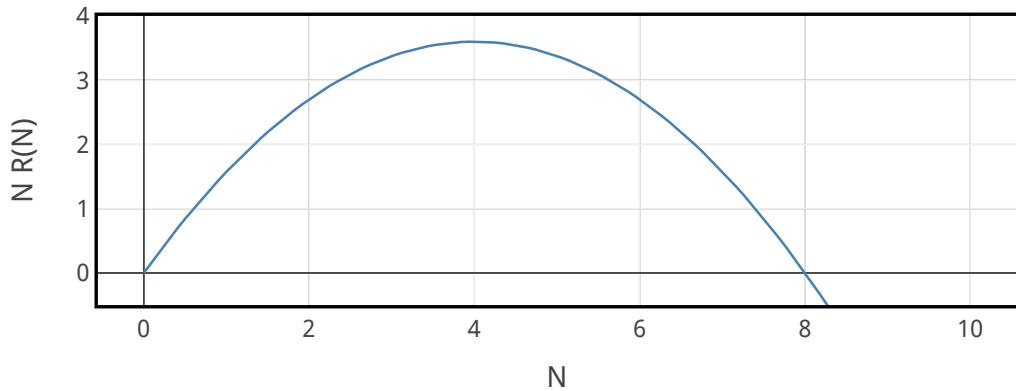
Fig. 1.6. $\dot{N}$ vs N for the logistic model. Here we chose $r = 1.8$ et $K = 8$.

Point 4: Trajectories. Cf. Figure 1.7.
Note that the slopes of the trajectories are constant on the horizontal lines $N = \text{const}$.
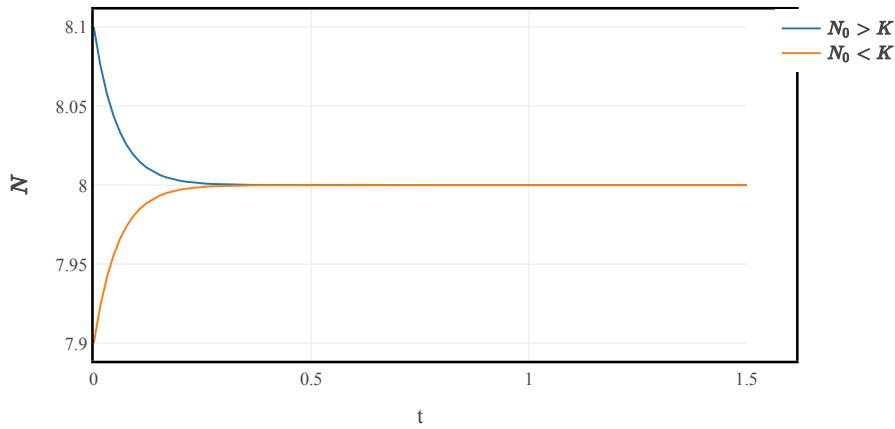
Fig. 1.7. Typical trajectories for the logistic model. Note the qualitative difference between an initial value $N_0 < K$ and $N_0 > K$. Here we chose $r = 1.8$ and $K = 8$.

### 1.4.3 Stability of the fixed points when $N = 0$ and $N = K$

Going back to Figure 1.6 we want to linearize the differential equation in a neighbourhood of the two fixed points:

Close to the fixed point $N^* = 0$ (i.e. for N_0 close to 0, cf. Fig. 1.8, the linearisation of the model is:

$$F(N) \approx F(0) + F'(0)(N - 0)$$

As $N = 0$ is a fixed point we have $F(0) = 0$:

$$\dot{N} = F'(0)N \quad \longrightarrow \quad N(t) = N_0 e^{F'(0)t} \tag{1.3}$$

Note that such approximation holds for both stable and unstable fixed points. Close to the fixed point $N^* = K$ (i.e. for N_0 close to K, cf. Fig. 1.8, the linearisation of the model is:

$$F(N) \approx F(K) + F'(K)(N - K)$$

As $N = K$ is a fixed point we have $F(K) = 0$, and changing variable $\eta = N - K$

$$\dot{\eta} = \dot{N} = F'(K)\eta \quad \longrightarrow \quad N(t) = K + (N_0 - K)e^{F'(K)t} \tag{1.4}$$

Note that such approximation again holds for both stable and unstable fixed points.

1.4.4 The logistic equation in population genetics

The logistic equation plays an important role in population genetics, since it describes, in a very simple situation, the temporal evolution of the frequency f of an allele subject to a selective advantage s in a haploid population of size N. It makes it possible to estimate the time scale that governs the fixation of such an allele, a phenomenon called "selective sweep".

A calculation of the frequency f of an allele that confers a relative advantage $1 + s$ in the rate of transmission of the number of individuals carrying this allele gives us the following equation logistics:

$$\dot{f} = sf(1 - f) \,.$$
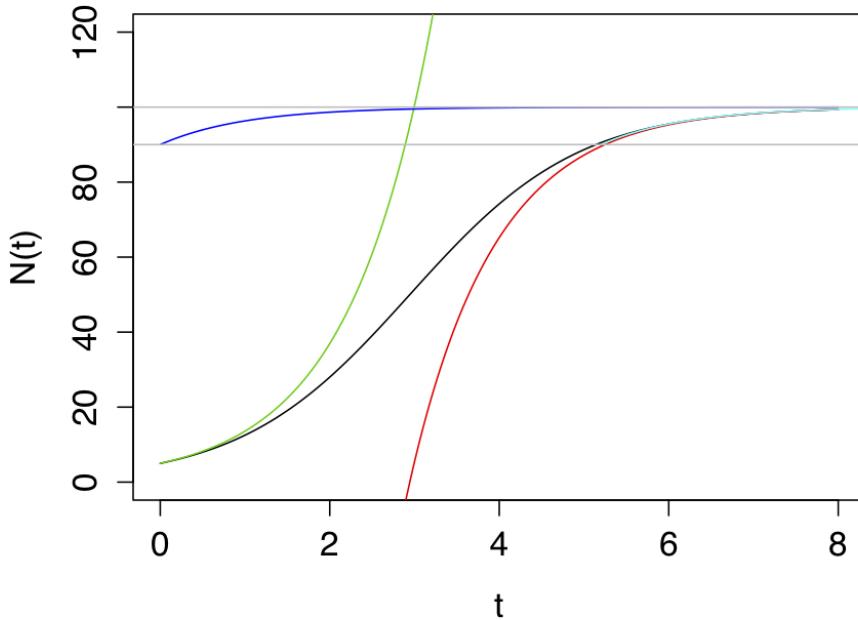
Fig. 1.8. Solution and approximations of the logistic equation. Here we have chosen $N_0 = 5$, $r = 1$ and $K = 100$. Black: exact solution; green: approximation of short times; red: approximation of long times (1.2); blue: linearization of the DS around the stable FP, with $N_0 = 90$; light blue: blue curve translated on the exact solution.

The derivation of this equation is based on the following considerations. Consider two alleles a and A represented by $N_a + N_A = N$ individuals. Consider also that the variations in the number of individuals carrying the alleles a and A follow (using continuous generations and assuming exponential growth):

$$\dot{N}_a = rN_a$$
$$\dot{N}_A = r(1+s)N_A,$$

where $r > 0$ is the relative growth rate for a, while A benefits from a selective advantage with a relative growth rate $r(1+s)$ where $s > 0$.

By introducing the allele A fraction f as $f = N_A/N$, we can compute the dynamics for the variables N and f, which results in:

$$\dot{N} = rN_a + r(1+s)N_A = rN(1+sf),$$
$$\dot{f} = \frac{\dot{N}_A}{N} - \frac{N_A}{N}\frac{\dot{N}}{N} = r(1+s)f - rf(1+sf) = rsf(1-f),$$

Therefore: $\dot{f} = rsf(1-f)$.

Note that the equation for f is decoupled from the one for N (but not vice versa). If we set $r = 1$, or if we use the change of variable $\tau = rt$, this equation becomes:

$$\dot{f} = sf(1-f).$$

By setting $x = \frac{f}{1-f}$ ($f = \frac{x}{1+x}$), we get $\dot{x} = sx$, and therefore:

$$f(\tau) = \frac{x_0\, e^{s\tau}}{1 + x_0\, e^{s\tau}} \; .$$

Fixation time for a new allele

If we consider a new allele of frequency $f_0 = 1/N_0$ ($x_0 \simeq 1/N_0$ for $N_0 \gg 1$), then

$$f(\tau) = \frac{e^{s\tau}}{N_0 + e^{s\tau}} \; , \tag{1.5}$$

which leads to the conclusion that the characteristic fixation time τ_{fix} (defined here as $e^{s\tau_{fix}} \approx N_0$) is given by

$$\tau_{fix} = \frac{\log(N_0)}{s} \; . \tag{1.6}$$

The dependency is therefore *logarithmix* in function of the population size.

For a population of $N_0 = 10^6$ et $s = 0.01$, we get $\tau_{fix} = 1000\, r^{-1}$ (i.e. in an order of magnitude of 1000 generations).

(R) This description is purely deterministic, and does not take into account the possibility that the allele A is randomly lost (genetic drift). A complete treatment must be done using a stochastic description.

2. A bistable biochemical switch in 1D

Some genes control their own expression. Here we will study a simplified model for the expression level of a self-induced gene g. This is also known as a positive feedback transcription factor. Typically g could be a transcription factor such as *pheromone-responsive Ste12 transcriptional regulator* in yeast; or HNF4α active in the liver and pancreas, mutations of which cause type I diabetes. The Oct4, Sox2 and Nanog genes, which are involved in maintaining the pluripotent state in stem cells, are also subject to such positive feedback.
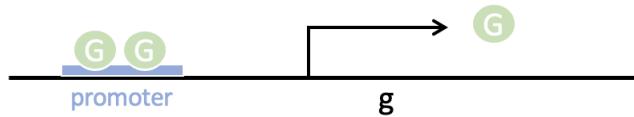
Fig. 2.1. Gene g with positive retro-feedback. Here the gene is activated by two binding sites for the protein G in its own promoter

.

2.1 Constructing the model

We would like to build a model for the concentration G of the protein from the gene g. The following hypothesis is made: The expression of the protein G closely follows that of the RNA messenger and therefore we will not model the RNA messenger explicitly.

Consider **three contributions**:

$$\dot{G} = \dot{G}_b + \dot{G}_d + \dot{G}_F,$$

I. Basal expression. It is assumed that the gene is expressed at a basal level independent of its expression level G.
$$\dot{G}_b = s_0$$

II. Degradation. It is assumed that the protein is degraded by a 1st order process (sometimes written $G \longrightarrow \emptyset$).
$$\dot{G}_d = -k_1 G$$

III. Positive feedback. The following hypothesis is made: The rate of expression of G is proportional to the bound fraction of the promoter $D_B(G)$ (B for "bound", D for "DNA").

$$\dot{G}_F = k_2 D_B(G)$$

How to calculate $D_B(G)$? Consider the following process:

- G binds its own promoter, here we consider that 2 adjacent binding sites are necessary.

- This reaction is rapid and can be treated at equilibrium (quasi-equilibrium).

We therefore write the reaction for protein-DNA binding:

$$2G + D_F \rightleftharpoons D_B$$

with the constraint $D_F + D_B = 1$ for a haploid gene. The subscripts refer to F (Free) and B (Bound); D stands for DNA. The equilibrium condition is written:

$$\dot{D}_B = q_1 G^2 D_F - q_{-1} D_B \approx 0 \qquad\qquad \rightarrow D_B(G) = D_B^* = \frac{G^2}{G^2 + \frac{q_{-1}}{q_1}}$$

Transcription is a highly complex and regulated process involving dozens or even hundreds of genes (in eukaryotes). The proposed model is therefore a rather simplification. It's a starting point.

To summarise, the complete model takes the form:

$$\dot{G} = \dot{G}_b + \dot{G}_d + \dot{G}_F = s_0 - k_1 G + k_2 \frac{G^2}{G^2 + K^2} \ ,$$

with $K = \sqrt{q_{-1}/q_1}$ the concentration at which the promoter is half occupied.

Dimensionless form

By introducing the variable $g = G/K$ and dividing by k_2, we obtain:

$$\frac{dg}{d\tau} = \frac{s_0}{k_2} - \frac{k_1 K}{k_2} g + \frac{g^2}{g^2 + 1}$$

$$\equiv s - r g + \frac{g^2}{g^2 + 1}$$

with $\tau = t k_2 / K$.

Why is dimensionless analysis useful? All the parameters are contained in the straight line $f(g) = s - r g$. The variables and parameters are dimensionless.

2.2 Analysis of model FPs

The aim is to determine the number and types of fixed points for each pair (s, r). This is also known as a *bifurcation diagram*. Here, we are interested in the case $r > 0, s > 0$.

Fixed points

To find the fixed points, let's say:

$$
\begin{aligned}
\frac{dg}{d\tau} &= F(g) \equiv -f(g) + h(g) = 0 \\
f(g) &= -s + rg \\
h(g) &= \frac{g^2}{g^2 + 1}
\end{aligned}
$$

and look for the points of intersection between $f(g)$ and $h(g)$.
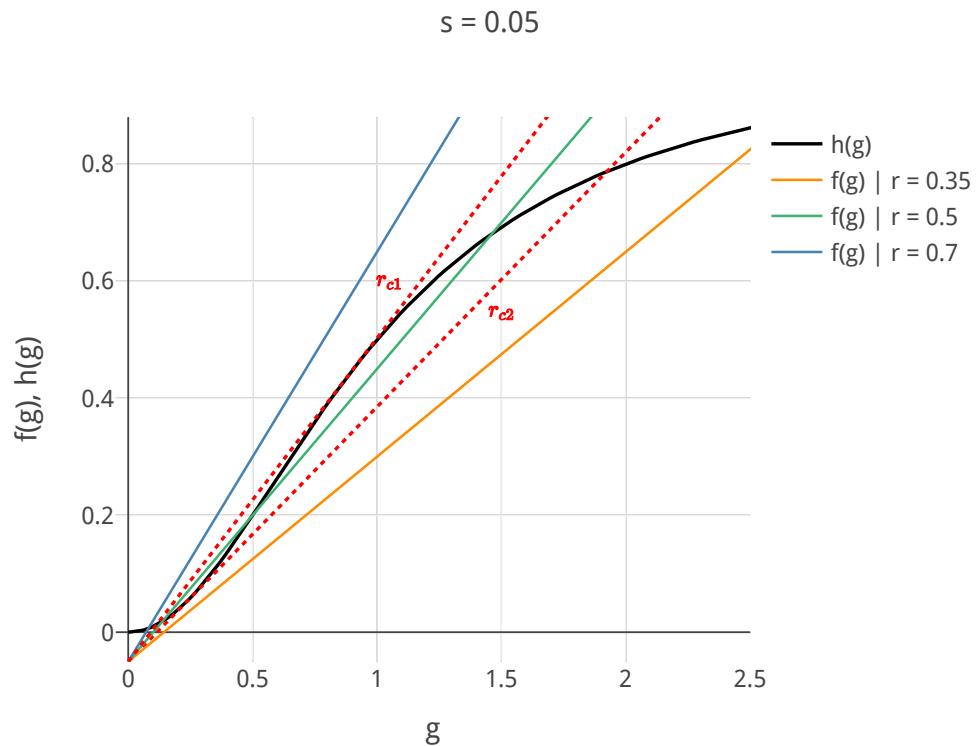
Fig. 2.2. $f(g)$ for different values of r for $s = 0.05$. $h(g)$ is fixed. r_{c1} and r_{c2} correspond to tangent cases. For $s < s_c$ fixed there are 5 cases: 1) pink: 1 fixed point (g^* large); 2) green: 3 fixed points; 3) light blue: 1 fixed point (g^* small); 4) red: borderline between 1) and 2) (r_{c2}); 5) blue: borderline between 2) and 3) (r_{c1}) .

The limiting cases (tangents r_{c1} and r_{c2}) are interesting because they delimit the regions with 1 or 3 fixed points. They correspond to points of *bifurcation* (Fig. 2.2). So let's set the conditions for finding these tangents:

$$(i)\ f(g) = h(g) \quad \text{and} \quad (ii) \quad f'(g) = h'(g) \Longrightarrow$$

$$r = \frac{2g}{(1+g^2)^2}$$

$$s = \frac{g^2(1-g^2)}{(1+g^2)^2} \ ,$$

and therefore r, s can be expressed as a function of g (parametric form) and define a curve in the (r, s) plane (Figure 2.4).

Calculation

- $(ii) \Rightarrow \quad -f'(g) = r = h'(g)$ does not depend on s.

- substitution of $r = \ldots$ in $(i) \Rightarrow s = \ldots$.

As $s(g)$ takes a maximum $s_c = 1/8$ in $g = 1/\sqrt{3}$, there are no tangent solutions for $s > s_c$, see Figs. 2.3 and 2.4).
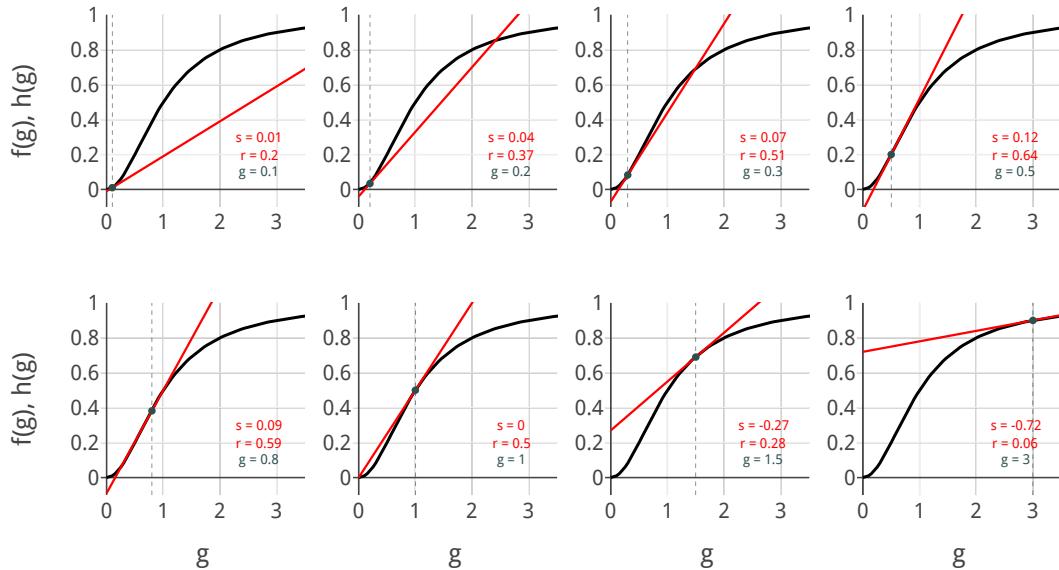
Fig. 2.3. Illustration of the tangent points. The red line represents $f(g, r(\tilde{g}), s(\tilde{g}))$ with $\tilde{g} = 0.1, \ldots, 3$ the tangent point. The solid black line represents $h(g)$. Note that s becomes negative from the seventh figure onwards

Stability of FPs

Geometrically, we can see from Figures 2.2 and 2.3 that for the g^* crossing points (the fixed points) we have:

- $F'(g^*) = -f'(g^*) + h'(g^*) < 0$ (stable) when a single fixed point is found, or for the two extreme FPs in cases with 3 fixed points.

- $F'(g^*) = -f'(g^*) + h'(g^*) > 0$ (unstable) for the central PF in cases with 3 fixed points.

Bifurcation diagram

The functions $r(g), s(g)$ are used to establish the bifurcation diagram in the (r,s) plane (Fig. 2.4).
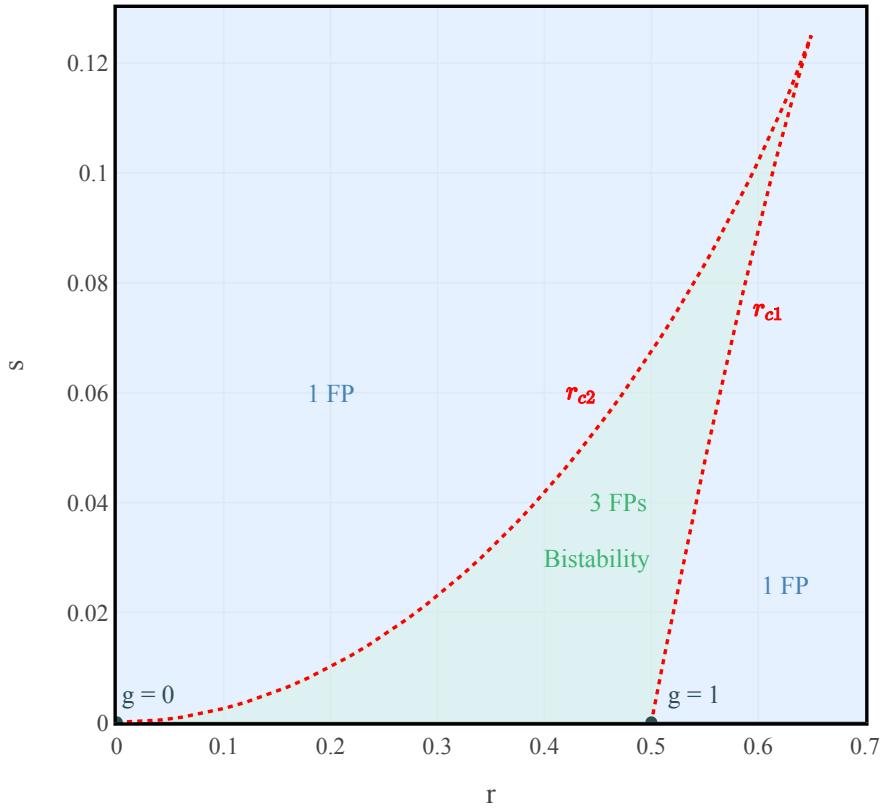
Fig. 2.4. Bifurcation diagram for $r, s > 0$. The red curve is parameterized by $(s(g), r(g))$ for $g \in [0,1]$, for $g > 1$ $s(g)$ becomes negative. The region in the horn comprises three fixed points, two of which are stable (bistable region). The single stable fixed point for r small corresponds to g^* large, and vice versa

.

Bistability, Memory and Hysteresis

Let's imagine a situation where r varies slowly and periodically from large to small as shown in Figure 2.5, while s is fixed. This could describe a situation where the protease concentration is under the control of the circadian clock (molecular clock with a period of 24 hours), e.g. r is a slow function of time $r(t) = \sin(2\pi/24[hr]\,t)$.
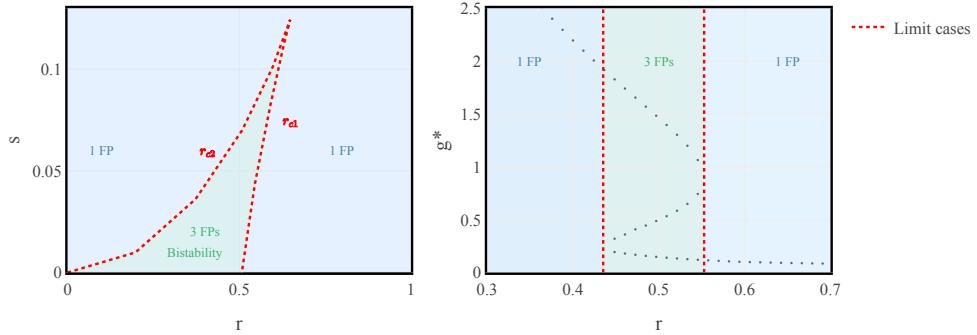

Fig. 2.5. Hysteresis. Left: Periodic variation of parameters in the (r, s) plane. Right: g^* as a function of r for a fixed s. $g^*(r)$ defines an "S" curve typical of a bistable system. The loop indicated by the arrows shows hysteresis behaviour.

Explanation: For $r > r_{c1}$ we have 1 fixed point: the gene is lowly expressed. Then r decreases and $r < r_{c1}$ but remains on the lower stable branch, even though the system now exhibits 3 fixed points. When $r > r_{c2}$ the lower stable fixed point disappears and gene expression suddenly increases towards the upper stable branch. Then a similar phenomenon (jump) occurs at r_{c1} as r decreases. With $r(t)$ periodic, the system then exhibits hysteresis loops around the "S" shown in Figure 2.5.

Exercise: Draw the trajectories $g(t)$ in the 3 typical regions.

3. 2D Linear systems, Linear Stability

2D non-linear systems show a much richer dynamic behaviour than 1D systems. They will make it possible to consider models of interacting populations, genetic systems, and highlight the possibility of oscillating solutions (limit cycles). Before tackling non-linear systems, which represent the cases of biological interest, we need to introduce the preparatory tools, i.e. study 2D linear systems.

A linear system in two dimensions is written:

$$\dot{x} = ax + by$$
$$\dot{y} = cx + dy \qquad \text{, where } a, b, c, d \text{ are real numbers.}$$

In matrix form:

$$\begin{pmatrix} \dot{x} \\ \dot{y} \end{pmatrix} = \begin{pmatrix} a & b \\ c & d \end{pmatrix} \begin{pmatrix} x \\ y \end{pmatrix}$$

and we will also use: $X = (x, y)$.

The aim is to characterise the trajectories $X(t) = (x(t), y(t))$ as a function of initial conditions (x_0, y_0).

3.1 Definitions

Most of the definitions will be the same (or easily generalised) for non-linear 2D systems.

3.1.1 fixed points

Definition 3.1.1 Fixed points are points (x^*, y^*) such that

$$(\dot{x} \; \dot{y}) = \begin{pmatrix} 0 \\ 0 \end{pmatrix} \text{ or in vector notation } \dot{X} = 0.$$

For the linear systems introduced above, $X^* = (0,0)$ is always a fixed point.

3.1.2 2D vector fields

Definition 3.1.2 This is the representation of the velocity vectors $(\dot{x}, \dot{y})$ in **the phase plane** (x, y).

There are two variants of representations:

- either the length of the vectors is fixed (often more practical)

- or it corresponds to the norm of the vector $(\dot{x}, \dot{y})$.

3.1.3 Isoclines

Definition 3.1.3 The isoclines represent the set of points defined by $\dot{x} = 0$ or $\dot{y} = 0$.

Linear systems are straight lines. The points of intersection between the isoclines $\dot{x} = 0$ and $\dot{y} = 0$ are fixed points.

3.1.4 Phase portraits in 2D

This is the representation of the trajectories $(x(t), y(t))$ in the phase plane.

Fundamental rules:

- Trajectories are tangent to the vector field at each point.
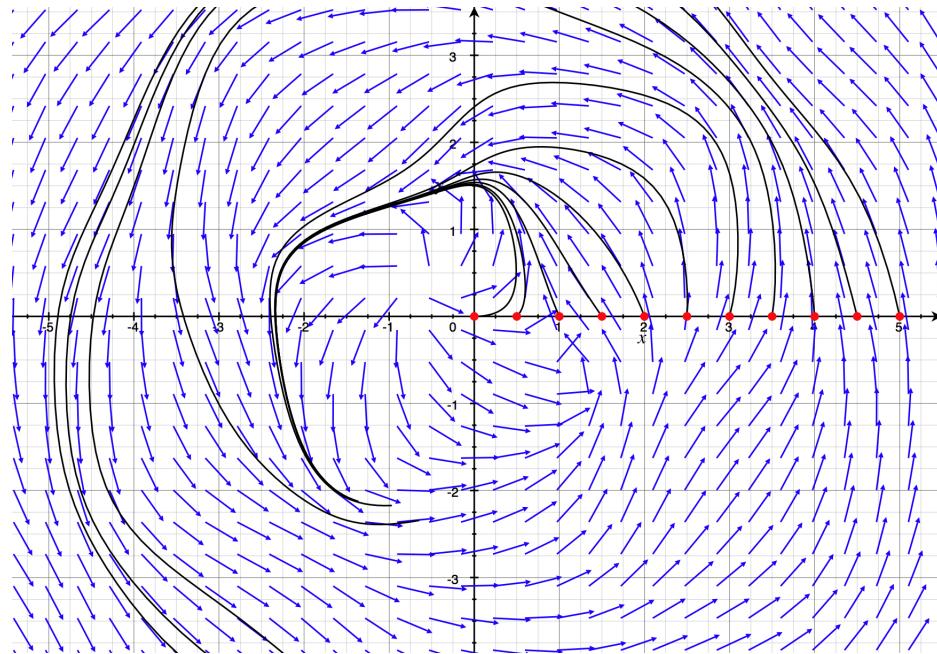
Fig. 3.1. Vector fields and 2D phase portrait. Generic example for a non-linear system.

- Two trajectories can touch but never cross (follows from the uniqueness theorem for solutions of differential equations: only **one** trajectory passes through any point which is not a fixed point).

3.1.5 Example

Let be the linear system

$$\begin{pmatrix} \dot{x} \\ \dot{y} \end{pmatrix} = \begin{pmatrix} a & 0 \\ 0 & -1 \end{pmatrix} \begin{pmatrix} x \\ y \end{pmatrix}$$

Here, we can also solve the system explicitly since it is decoupled:

- $\dot{x} = ax \longrightarrow x(t) = x_0\, e^{at}$

- $\dot{y} = -y \longrightarrow x(t) = y_0\, e^{-t}$

We see that an initial condition on an axis (x or y) remains on this axis for any time t.

Case a=1

A. Sketch of the vector field for $a = 1$:

1. Start by drawing the vector field on **isoclines**.

- $\dot{x} = 0 \Rightarrow x = 0$ and so the velocity vectors on this line are purely in the y direction. What's more, they have the opposite sign to y and become longer and longer as we move away from the origin.

- $\dot{y} = 0 \Rightarrow y = 0$ and so the velocity vectors on this line are purely in the x direction.

2. Then determine **the direction of the velocities** in the regions delimited by the isoclines. In these regions, in this case quadrants I, II, III and IV, the velocity components have the same sign.

B. Trajectory sketch
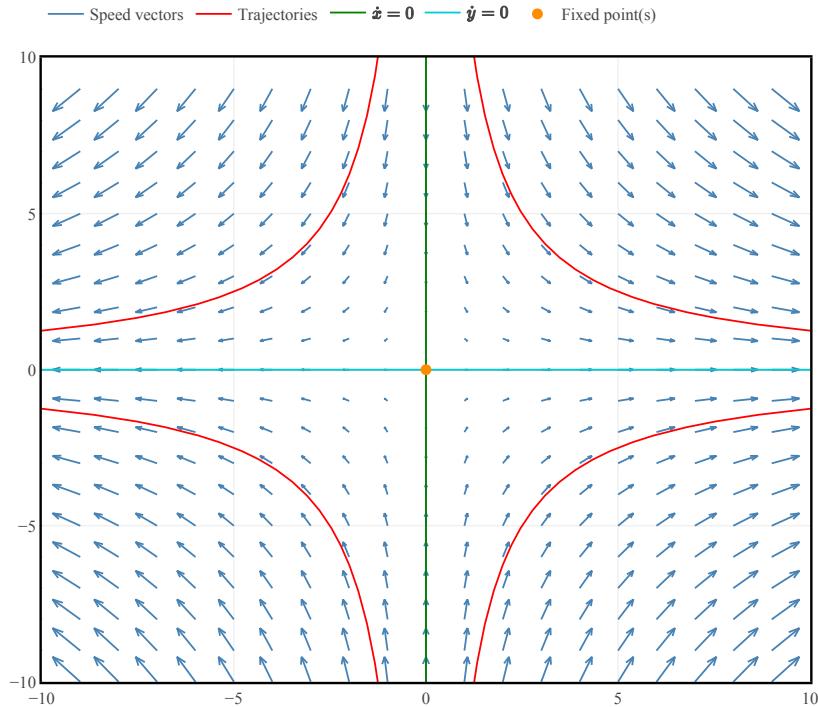
Fig. 3.2. Vector fields for $a = 1$. This is the prototypical case of a **Saddle point**. Cf. sections 3.2 and the systematic classification 3.2.2. Some typical trajectories are shown in red

3. Following tangents

The following other cases are found as a function of a (Fig. 3.3):

- $a > 0$: **Saddle point**. A stable direction (y) and an unstable direction (x) .

- $a = 0$: marginal case with $x(t) =$const. There is a line of fixed points.

- $-1 < a < 0$. **Stable fixed point** (stable node). The y direction decreases faster than the x direction; x is the slow direction.

  – For $t \to \infty$ the trajectories are parallel to the x axis.
  – For $t \to -\infty$ they are parallel to y.

- $a = -1$. Stable star node.

- $a < -1$. **Stable fixed point** (stable node). It is now the x direction that decreases faster than y.

Cas 1 : a > 0   **Cas 2 : a = 0**

Cas 3 : -1 < a < 0   **Cas 4 : a = -1**

Cas 5 : a < -1

— Vecteurs vitesse
— Trajectoires
— $\dot{x} = 0$
— $\dot{y} = 0$
● Point(s) fixe(s)
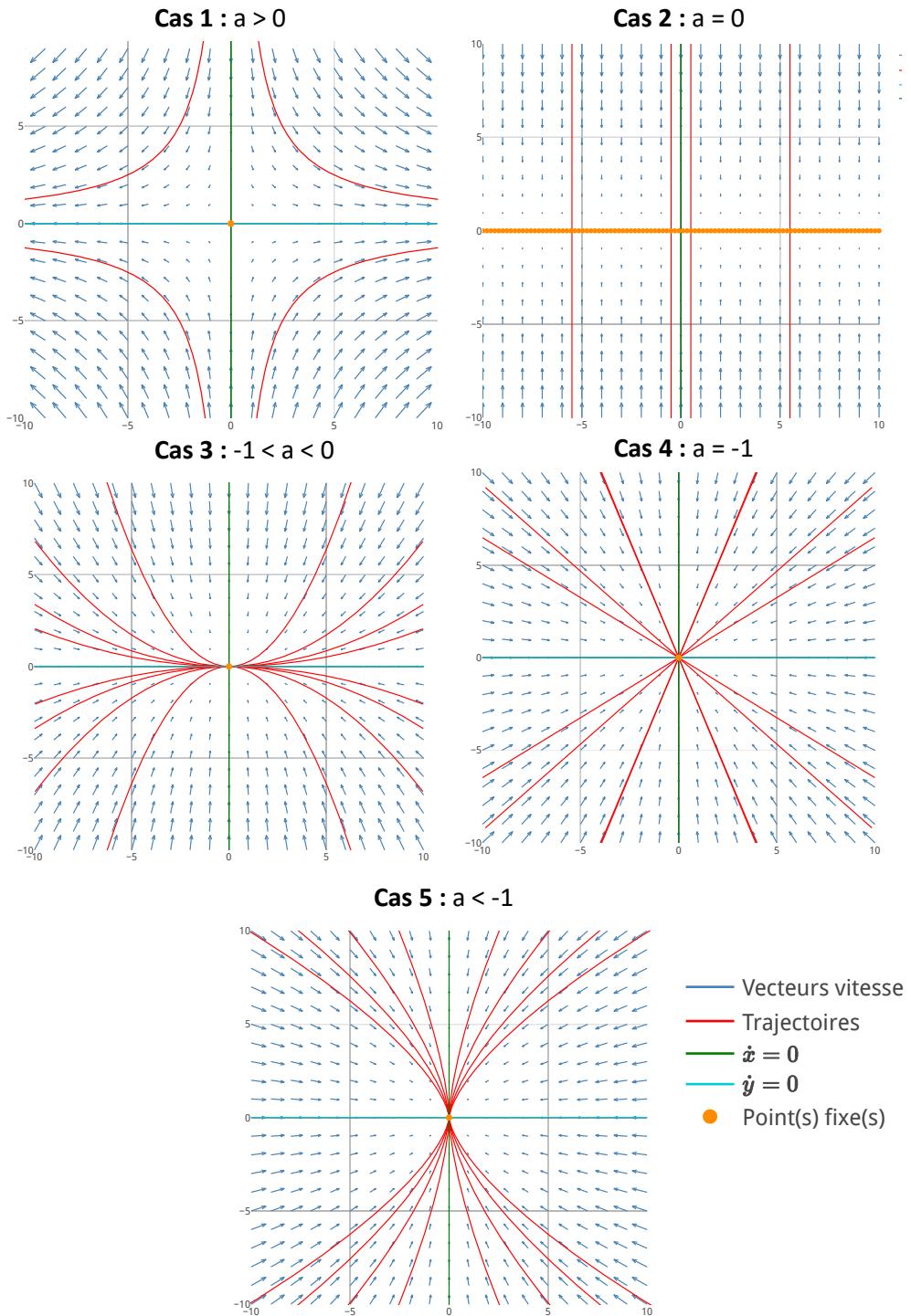
Fig. 3.3. Vector fields for different parameter values:
• **Case** $a > 0$**:** Saddle point.
• **Case** $a = 0$**:** Line of fixed points.
• **Case** $-1 < a < 0$**:** Fixed point (star node). Slow direction: x.
• **Case** $a = -1$**:** Stable FP, star node.
• **Case** $a < -1$**:** Stable FP. Slow direction: y.

3.2 Solutions and stability analysis

3.2.1 General solution

The general solution for

$$\begin{pmatrix} \dot{x} \\ \dot{y} \end{pmatrix} = \begin{pmatrix} a & b \\ c & d \end{pmatrix} \begin{pmatrix} x \\ y \end{pmatrix} \equiv M \begin{pmatrix} x \\ y \end{pmatrix} \tag{3.1}$$

is written as

$$X(t) = c_1 v_1 e^{\lambda_1 t} + c_2 v_2 e^{\lambda_2 t}$$

where:

- λ_1, λ_2 and v_1, v_2 are the eigenvalues and eigenvectors of the matrix M.

- this solution applies when $\lambda_1 \neq \lambda_2$ (for the case $\lambda_1 = \lambda_2$, see below.)

- c_1, c_2 are constant coefficients fixed by the initial conditions. They are the projections of the initial condition onto v_1 and v_2.

Note: All these quantities can take complex values.

Interpretation: c_1 and c_2 are the coefficients of the vector $X(t=0)$ in the basis (v_1, v_2). The basis is typically non-orthogonal, except in special cases.

Proof that the formula is the correct solution :

$$MX(t) = c_1 e^{\lambda_1 t} M v_1 + c_2 e^{\lambda_2 t} M v_2 = c_1 e^{\lambda_1 t} \lambda_1 v_1 + c_2 e^{\lambda_2 t} \lambda_2 v_2 = \dot{X}(t)$$

Corollaries:

- An initial condition on a proper direction remains on this direction for all time.

- The FP $(0,0)$ is stable if and only if $\text{Re}(\lambda_i) < 0$ for $i = 1, 2$.

Linear algebra reminder

The characteristic equation $\det(M - \lambda I) = 0$ gives $\lambda^2 - \tau \lambda + \Delta = 0$, with $\Delta = ad - bc$ the determinant and $\tau = a + d$ the trace of M. The determinant and the trace are invariants (independent of the basis) and are therefore expressed in terms of the eigenvalues as $\tau = \lambda_1 + \lambda_2$ and $\Delta = \lambda_1 \cdot \lambda_2$.

Example: $\begin{pmatrix} 1 & 1 \\ 4 & -2 \end{pmatrix}$ has eigenvalues $\lambda_1 = 2, \lambda_2 = -3$ and the associated vectors are $v_1 = (1, 1)$ and $v_2 = (1, -4)$.

So the system $\dot{X} = MX$ takes as its solution

$$\begin{pmatrix} x(t) \\ y(t) \end{pmatrix} = \begin{pmatrix} c_1 e^{2t} + c_2 e^{-3t} \\ c_1 e^{2t} - 4c_2 e^{-3t} \end{pmatrix} ,$$

where c_1, c_2 are to be fixed according to the initial condition (cf Figure 3.4)
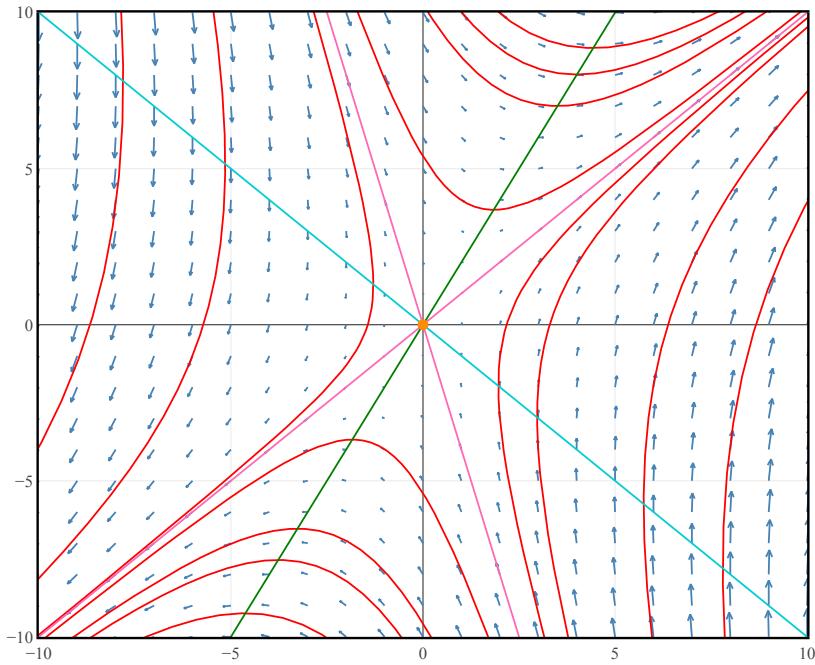
Fig. 3.4. Sketch of the phase portrait. The proper directions are in purple

.

Matrix exponential in 2D

Note: this section may be omitted on first reading. However, the result is most interesting.
The solution to the equation (3.1) can also be calculated as a matrix exponential. As a corollary
of the Cayley-Hamilton theorem (linear algebra), it is possible to write any matrix function, for a
matrix A of dimension $n \times n$, as a matrix polynomial in A of dimension $n-1$. Surprising but true!
For the matrix exponential in 2D, the expression is as follows:

$$e^{tA} = e^{st} \left(\left(\cosh(qt) - s \frac{\sinh(qt)}{q} \right) I + \frac{\sinh(qt)}{q} A \right) ,$$

or $s = \frac{\text{trace}(A)}{2} = \frac{\alpha+\beta}{2}$ and $q = \frac{\alpha-\beta}{2}$, with α and β the eigenvalues of the matrix. Furthermore,
$q^2 = s^2 - \det(A)$.

3.2.2 Classifying the stability of FPs from the determinant and the trace of the M matrix

We can effectively classify the stability of fixed points for models according to the trace and determinant of the M matrix. (Figure 3.5).

Case 1. $\Delta < 0$: Saddlepoint. It follows that the eigenvalues are real and of opposite sign.

Case 2. $\Delta > 0$ and $\tau < 0$: Stable fixed point.

Case 2a. If $\tau^2 - 4\Delta > 0$ we find a stable node.

Case 2b. If $\tau^2 - 4\Delta < 0$ we find a stable spiral (the eigenvalues are complex). $2\lambda_{1,2} = \tau \pm i\sqrt{||\tau^2 - 4\Delta|}$ are complex conjugates.
Why is it spinning? Because of the complex eigenvalues. $e^{(a+ib)t} = e^{at}(\cos(bt) + i\sin(bt))$ with $a = 2\tau$ and $b = 2\sqrt{|\tau^2 - 4\Delta|}$, we therefore obtain an exponential spiral of frequency b.

Case 3. $\Delta > 0$ and $\tau > 0$: Unstable fixed point.

Case 3a. If $\tau^2 - 4\Delta > 0$ we find an unstable node.

Case 3b. If $\tau^2 - 4\Delta < 0$ we find an unstable spiral (complex eigenvalues).

Some special cases. $\lambda_1 = \lambda_2 = \lambda$ $(\tau^2 - 4\Delta = 0)$.

Case a. the dimension of the space associated with λ is **two**. We find a star-shaped fixed point, stable or unstable (see Fig. 3.3, Case 4). $X(t) = X_0 e^{\lambda t}$.

Case b. the dimension of the space associated with λ is **one**. We find a stable $(\tau < 0)$ or unstable $(\tau > 0)$ degenerate fixed point.

For more details on the special cases $\Delta = 0$, $\tau = 0$, and $\tau^2 - 4\Delta = 0$, see Strogatz's book.
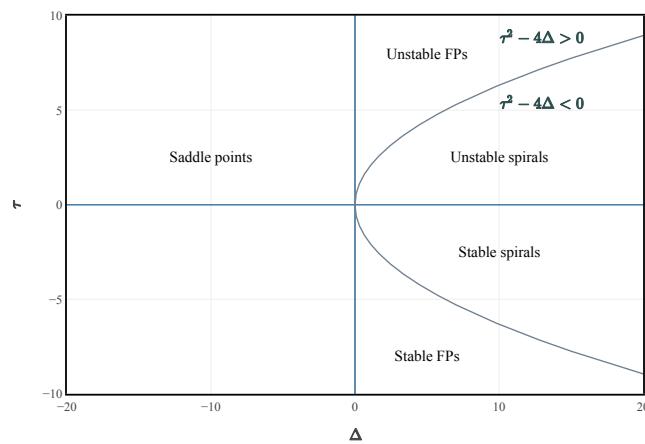

Fig. 3.5. Representation of stability regions in the (Δ, τ) plane
.

3.2.3 Establish phase portraits around fixed points

Use 4 directions (only 2 in the case of spirals):

- 2 isoclines

- 2 directions: the eigenvectors of the M matrix (spirals give complex eigenvectors which cannot be represented as directions)

A. Stable fixed points: $\Delta > 0$ and $\tau < 0$. Order the eigenvalues such that $\lambda_2 < \lambda_1 < 0$. Then v_2 is called the fast direction because it decreases faster than v_1.

1. The trajectories for $t \to \infty$ tend towards the fixed point tangentially to the slow direction v_1.

2. The trajectories for $t \to -\infty$ are parallel to the fast direction v_2.

Examples: Fig. 3.6.
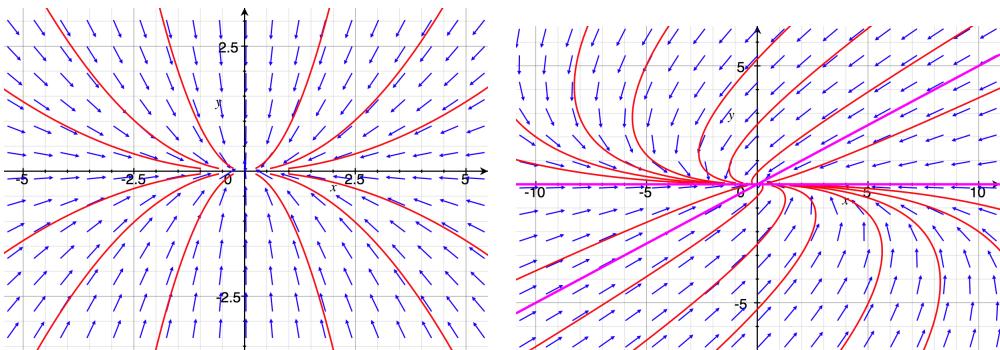
Fig. 3.6. Stable fixed point. Left: $v_1 \perp v_2$. Right: general case. The eigen directions are in violet. The slow direction is $v_1 = (1,0)$ in both cases

.

B. Unstable fixed points: $\Delta > 0$ and $\tau > 0$. Let's order the eigenvalues such that $0 < \lambda_1 < \lambda_2$: v_2 is called the fast direction because it grows faster than v_1.

- The trajectories for $t \to -\infty$ tend towards the fixed point tangentially to the slow direction v_1. The trajectories move away from zero tangent to the slow direction.

- The trajectories for $t \to \infty$ diverge parallel to the fast direction v_2.

Example: As for case A but reversing the direction of the trajectories.

C. Saddle points: $\Delta < 0$. Order the eigenvalues such that $\lambda_2 < 0, \lambda_1 > 0$. v_1 is called the unstable direction and v_2 the stable direction. Drawing the phase portrait for this case is less difficult.

D. Spirals. To determine the direction of rotation, draw the vector fields on the isoclines. **Example:** (see series 5, exercise 1)

E. Stable degenerate fixed points. As for the other stable FPs, use the isoclines and the vector field.

- The trajectories for $t \to +\infty$ tend towards the fixed point tangent to the proper direction v.

- The trajectories for $t \to -\infty$ diverge parallel to the proper direction v.
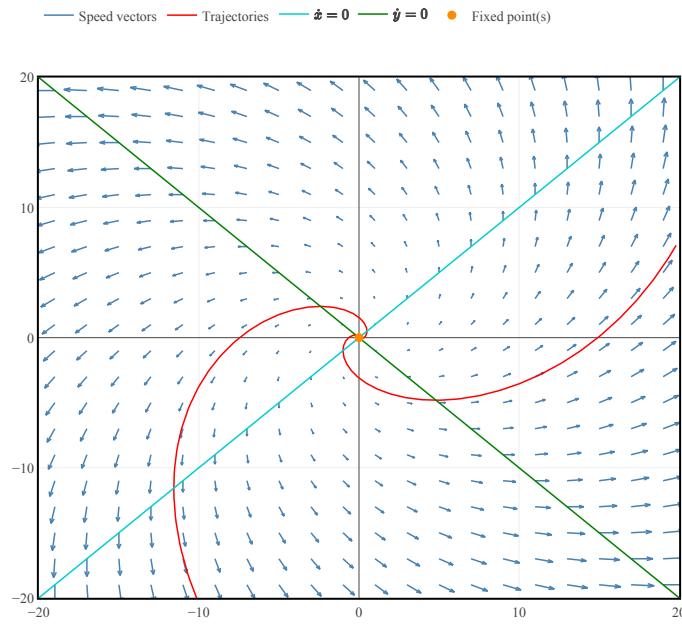
**Fig. 3.7.** Unstable spiral for $M = (1 \; -1; \; 1 \; 1)$ with isoclines in green and light blue
.

F. Unstable degenerate fixed points. Similar.

Note: The eigenvalues and eigenvectors are real except for cases 1b and 2b (spirals).

4. Nonlinear 2D systems: predator-prey models

Predator-prey models describe two interacting populations. They are often used in ecology or population dynamics to highlight phenomena such as temporal oscillations. The formalism developed can be applied in the same way to chemical reactions or two-component gene networks.

4.1 Analysis of 2D non-linear systems

A typical example of a 2D phase portrait is shown in Fig. 4.1.

A. Vector fields (CV) for 2D non-linear systems

- Same as in the linear case: draw the "velocities" $(\dot{x}, \dot{y})$ at each point of the phase plane (x, y).
- Caution: isoclines can be *curves* and can also have several branches.

B. Phase portraits. This is the representation of the trajectories $(x(t), y(t))$ in the (x, y) plane.

Important: Trajectories in the phase plane never intersect. Complex phase portraits (with several fixed points) can be understood as locally linear systems "glued together."
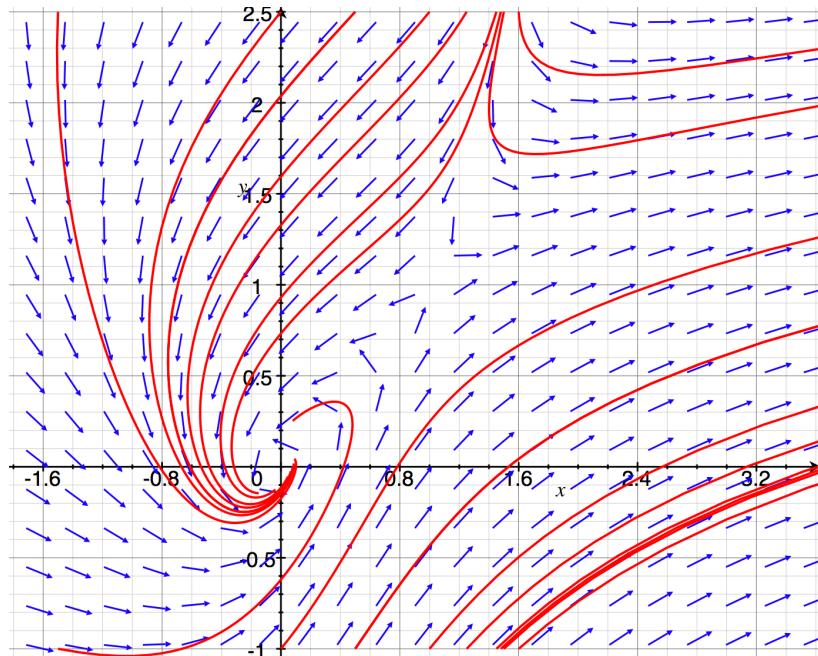
Fig. 4.1. A typical phase portrait: a saddle point and a spiral
.

C. Fixed points and linearisation around fixed points. The set of points (x^*, y^*) such that $F(x^*, y^*) = 0$ are the fixed points of the system. To study the behaviour in the vicinity of a fixed point we use a 2D series expansion. We pose $u = x - x^*, v = y - y*$, from which it follows:

$$\dot{u} = f_1(x, y) = f_1(u + x^*, v + y^*) = f_1(x^*, y^*) + u\frac{\partial f_1}{\partial x} + v\frac{\partial f_1}{\partial y} + \mathscr{O}(u^2, v^2, uv)$$

$$\dot{v} = f_2(x, y) = f_2(u + x^*, v + y^*) = f_2(x^*, y^*) + u\frac{\partial f_2}{\partial x} + v\frac{\partial f_2}{\partial y} + \mathscr{O}(u^2, v^2, uv) \, ,$$

or, since $(f_1(x^*,y^*) = f_2(x^*,y^*) = 0)$, in vector writing :

$$\begin{pmatrix} \dot{u} \\ \dot{v} \end{pmatrix} = J \begin{pmatrix} u \\ v \end{pmatrix} \quad \text{with} \quad J = \begin{pmatrix} \frac{\partial f_1}{\partial x} & \frac{\partial f_1}{\partial y} \\ \frac{\partial f_2}{\partial x} & \frac{\partial f_2}{\partial y} \end{pmatrix}\bigg|_{(x^*,y^*)} = J(x^*,y^*)$$

the Jacobian at the point (x^*,y^*).

And so we end up with an <u>linear 2D</u> problem as in Chapter 3.

4.2 Predator-Prey Models

Predator-prey models represent a class of generic models which describe the dynamics of 2 populations (animals, chemical species, etc) interacting.

Here, we want to describe 2 populations, the preys n and the predators p in an environment with finite capacity. The model takes elements from the logistic growth model.

Model

$$\dot{n} = an(1 - \frac{n}{K_n}) - bnp$$

$$\dot{p} = -cp + dp\left(n - \frac{p}{K_p}\right) = -cp + dnp\left(1 - \frac{p}{nK_p}\right)$$

Interpretation

- Without predators $(p = 0)$, the preys n follows a logistic growth.

- The product n, p is proportional to the probability of encounter between predators and preys.

- The preys n disappear at a rate proportional to the number of encounters between preys and predators (b).

- Predators die in the absence of prey $(-c)$.

- Note: the capacity of the environment for predators depends on the number of preys: $p^* = nK_p$.

We redefine the parameters to obtain

$$\dot{n} = n(a - en - bp)$$
$$\dot{p} = p(-c + dn - fp)$$

with all constants > 0.

Analysis of the model

We restrict ourselves to quadrant Q1 with (n, p) positive (the populations are positive).

Isoclines

$$\dot{n} = 0 \longrightarrow en + bp = a \quad \text{or} \quad n = 0$$
$$\dot{p} = 0 \longrightarrow dn - fp = c \quad \text{or} \quad p = 0$$

Case A: $\frac{a}{e} < \frac{c}{d}$.

Here, there is no crossing of the isoclines in Q1. Therefore, we find 2 fixed points $(0,0)$ and $P = (\frac{a}{e}, 0)$.

How do you find the sign of the velocity vectors in the different regions I, II, III?

- <u>Method 1:</u> Choose values for n, p and use the formulas for $\dot{n}$ and $\dot{p}$.
- <u>Method 2:</u> Consider $\dot{n} = n(a - en - bp)$. For p fixed and n large the term $-en^2$ dominates and therefore the region above the line $D1$ corresponds to $\dot{n} < 0$ (regions I,II). Consequently the region below this line corresponds to $\dot{n} > 0$ (region III). Then idem for $\dot{p}$.
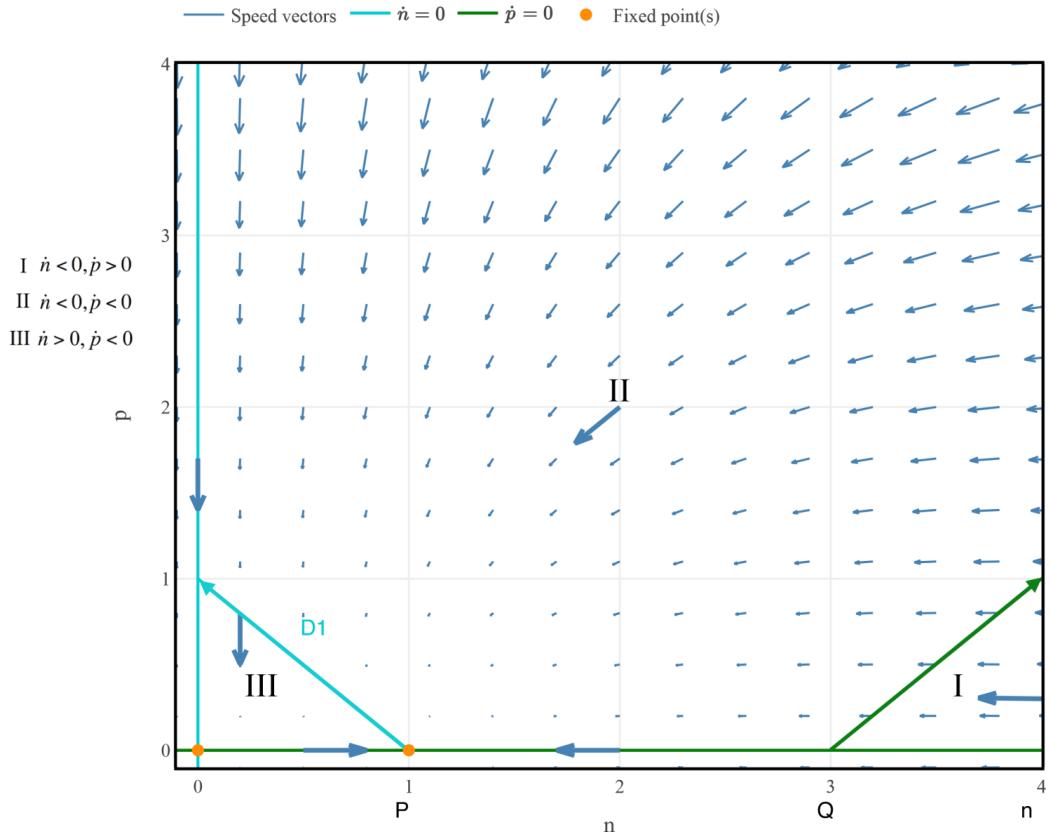
Fig. 4.2. Isoclines and vector fields for case A. $P = (a/e, 0)$, $Q = (c/d, 0)$.

Stability of fixed point (0,0)

The Jacobian at this point is

$$J = \begin{pmatrix} a - 2en - bp & -bn \\ dp & -c + dn - 2fp \end{pmatrix} \Rightarrow J(0) = \begin{pmatrix} a & 0 \\ 0 & -c \end{pmatrix}$$

with eigenvalues/eigenvectors:

$$\lambda_1 = a > 0 \, ; v_1 = (1,0) \quad \text{and} \quad \lambda_2 = -c < 0 \, ; v_2 = (0,1)$$

So the fixed point $(0,0)$ is a saddle point.

Stability of fixed point P = (1,0)

$$J(P) = \begin{pmatrix} -a & -b\frac{a}{e} \\ 0 & -c + d\frac{a}{e} \end{pmatrix}$$

with the eigenvalues/eigenvectors:

$$\lambda_1 = -a < 0 \, ; v_1 = (1,0) \quad \text{and} \quad \lambda_2 = -c + d\frac{a}{e} < 0 \, ; v_2 \quad \text{depends on parameters.}$$

Consequently the fixed point P is stable in case A. The phase portrait depends on the parameters. For example for $(a = b = d = e = f = 1, c = 3)$ the Jacobian $J(P) = \begin{pmatrix} -1 & -1 \\ 0 & -2 \end{pmatrix}$, the slow direction is $v_1 = (1,0)$ and $v_2 = (1,1)$.
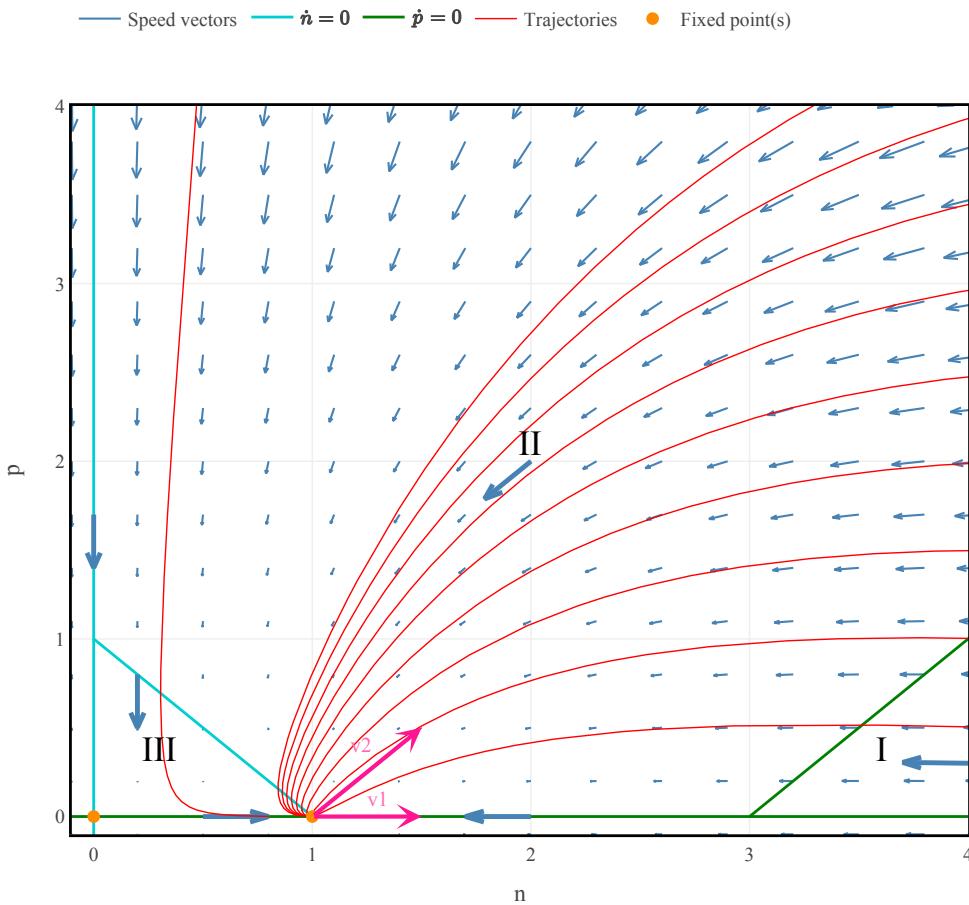
Fig. 4.3. Phase portrait for case A. The trajectories are in red.

Conclusion for case A: We observe the extinction of predators in the FP.

Case B: $\frac{a}{e} > \frac{c}{d}$.

Here we find a crossing of the isoclines in Q1.
There are 3 fixed points $(0,0)$, P and the intersection $I = \left(\frac{af+bc}{bd+ef}, \frac{ad-ec}{bd+ef}\right)$.

Stability of $(0,0)$**:** Idem Case A.
Stability of P**:**

$$J(P) = \begin{pmatrix} -a & -b\frac{a}{e} \\ 0 & -c+d\frac{a}{e} \end{pmatrix}$$

with the eigenvalues/eigenvectors:

$$\lambda_1 = -a < 0 ; v_1 = (1,0) \quad \text{and} \quad \lambda_2 = -c + da/e > 0 .$$
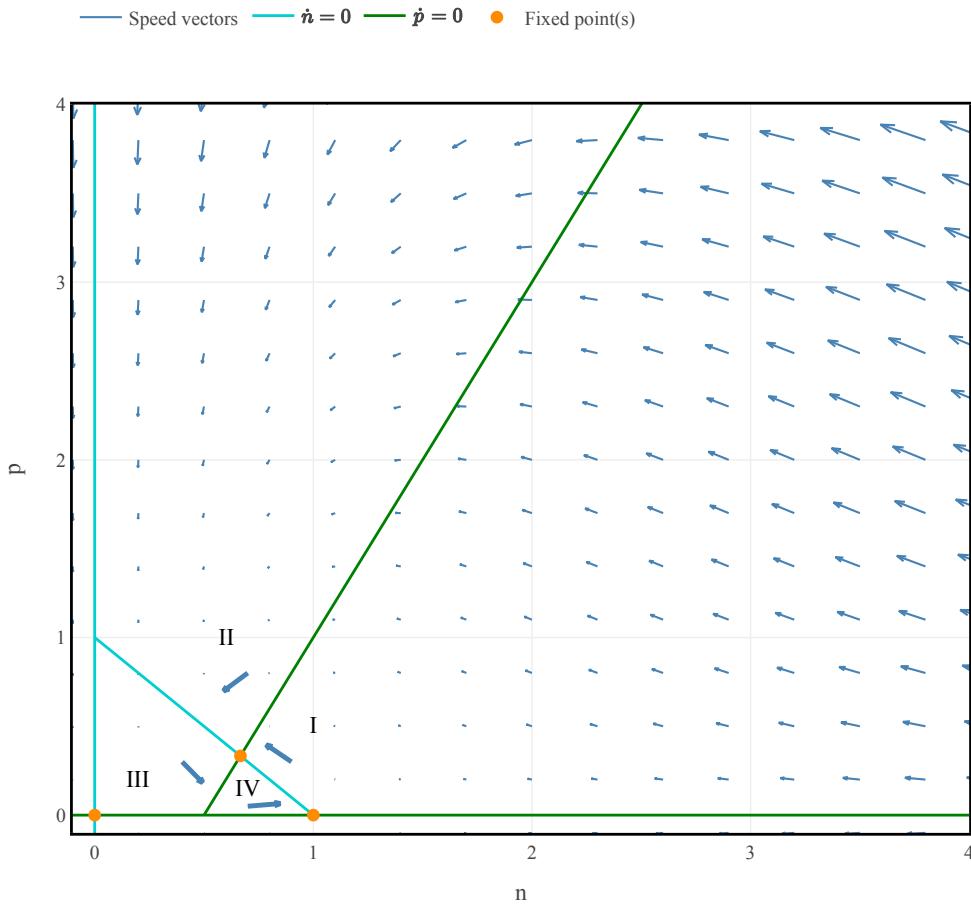
Fig. 4.4. Isoclines and vector fields for case B.

So the fixed point P is a saddle point. Let's consider an example ($a = e = b = c = f = 1, d = 2$), in this case $v_2 = (1, -2)$.

Stability of I: For ($a = e = b = c = f = 1, d = 2$) the point $I = (2/3, 1/3)$ and

$$J(I) = \frac{1}{3} \begin{pmatrix} -2 & -2 \\ 2 & -1 \end{pmatrix}$$

with $\tau = -1, \Delta = 2/3 \Rightarrow 2\lambda_{1,2} = -1 \pm i\sqrt{5/3}$. The fixed point is therefore a stable spiral.

<u>**Conclusion**</u> for case B: The ecosystem tends towards an equilibrium between the 2 populations, and this is achieved by oscillations of decreasing amplitude.
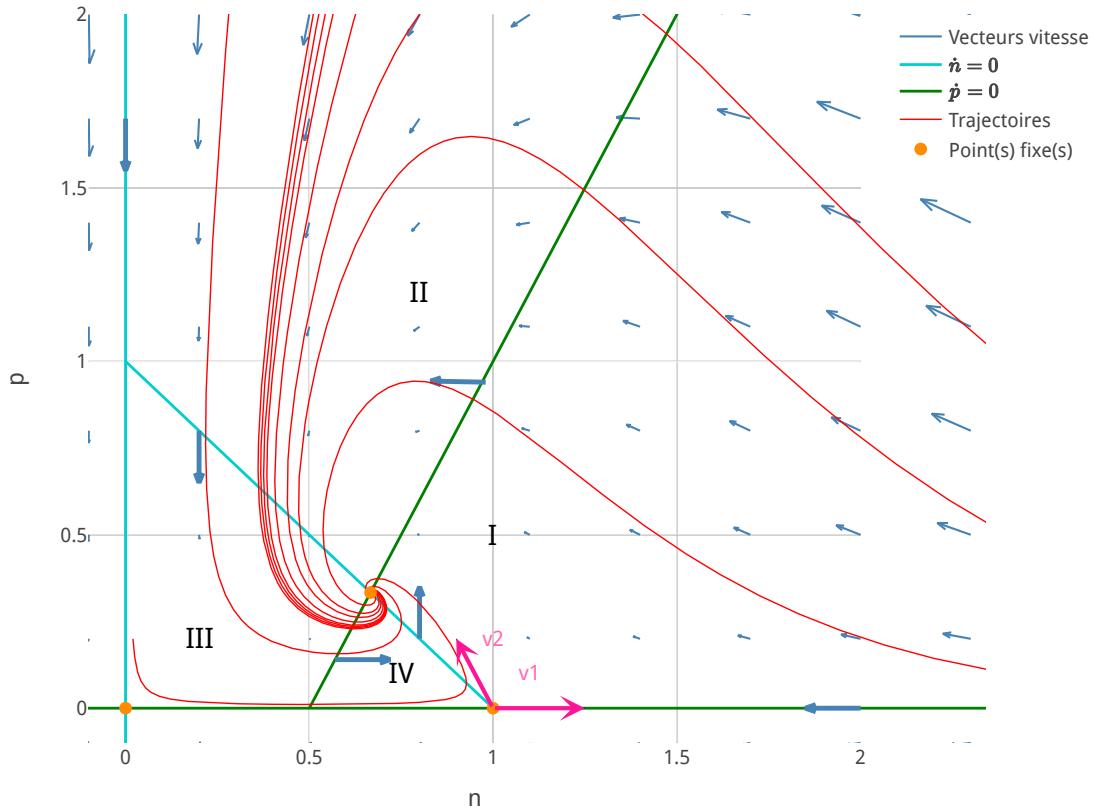
Fig. 4.5. Phase portrait for case B.

4.3 Case study: Construction of a genetic toggle switch in E. coli

The aim is to study an example where the modelling of a two-component genetic network is used to aid the construction of a synthetic switch. Synthetic biology is the branch of biology that uses modelling to design genetic networks with a predefined behaviour, for example an oscillator or a switch.

The course consists of a reading of the paper by Gardner, Cantor and Collins (Nature 2000). See also the appendix file CHAPTER 4.3.pdf.

5. Biological oscillators

Molecular oscillators are common in biology. Here are a few examples, some of which will be covered in the course and exercises:

- cell cycle

- glycolysis cycle

- action potentials: periodic discharges in neurons

- circadian clock

and others that we won't have time to go into, such as

- somite formation clock in vertebrates

- respiration cycle in yeast (metabolic oscillations).

Oscillations in an autonomous and isolated dynamic system are only possible in dimension $d > 1$.

5.1 Limit cycle oscillators

5.1.1 Definitions

A. A limit cycle $O(t)$ is an isolated, periodic (i.e. self-closing) trajectory of period T: $O(t+T) = O(t)$. This means that nearby trajectories are not closed but move towards or away from O. No point on $O(t)$ is a fixed point.

B. O is stable if it attracts nearby trajectories, or unstable if it repels them.

C. There are also semi-stable limit cycles (rare).
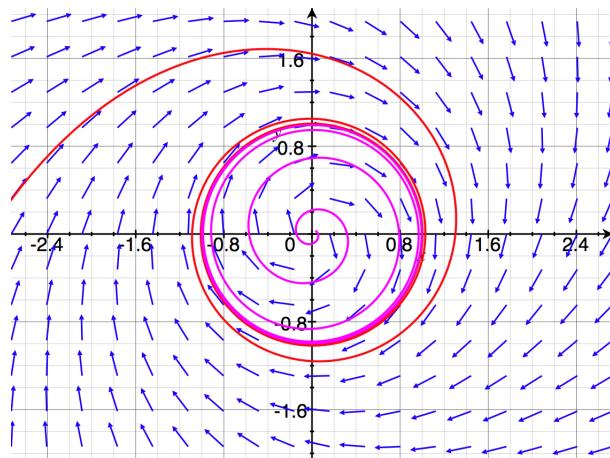
Fig. 5.1. Stable limit cycle in $r = 1$.

Properties:

- A limit cycle necessarily encircles at least one stable or unstable fixed point (spirals are also permitted).

- There cannot be a limit cycle around a single saddle point.

Example:

$$\begin{pmatrix} \dot{x} \\ \dot{y} \end{pmatrix} = \begin{pmatrix} -y + x(1 - x^2 - y^2) \\ x + y(1 - x^2 - y^2) \end{pmatrix} \ .$$

or written in polar coordinates:

$$\begin{pmatrix} \dot{r} \\ \dot{\phi} \end{pmatrix} = \begin{pmatrix} r(1 - r^2) \\ 1 \end{pmatrix} \quad , \quad r^2 = x^2 + y^2 \ .$$

Since $r^* = 1$ is a stable fixed point of the radial equation, $(x(t), y(t)) = (\cos(t), \sin(t))$ is a stable limit cycle. The phase portrait is shown in Figure 5.1.

5.1.2 Criteria for the presence of limit cycles

In general, it is not easy to prove the existence of a limit cycle. In practice, we usually use simulations (see exercises). However, there is a very useful theorem defining the conditions for the existence of a limit cycle.

Poincaré-Bendixon Theorem (PBT)

A. A (<u>stable</u>) limit cycle (an attractor) exists in a region R bounded by a closed (simple) curve if :

  – The vector field everywhere on the edge of R points towards the interior of the region (R is called a confinement or trapping region)

  – R contains exactly one unstable fixed point (or one unstable spiral)

B. An (<u>unstable</u>) limit cycle(a repeller) exists in a region R bounded by a closed (simple) curve if :

  – The vector field everywhere on the edge of R points outside the region

 – R contains exactly one stable fixed point (or stable spiral)
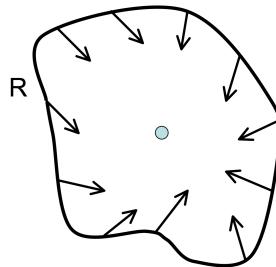
Fig. 5.2. The Poincaré-Bendixson theorem requires the existence of a confinement region on the edge of which the vector field points inwards (for a stable limit cycle). The region must also contain a fixed (unstable) point.

5.2 Glycolysis cycle

A. Motivation The glycolysis cycle allows the PBT theorem to be applied. Glycolysis is the conversion of glucose into pyruvate (10 enzymes in all, cf. Figure 5.3), and can be summed up in the net reaction:5.3.

$$\text{Glucose} + 2ADP + 2Pi \longrightarrow 2\,\text{Pyruvate} + 2ATP\ .$$
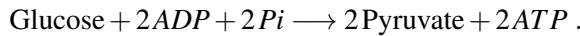
During fermentation, pyruvate is then broken down into lactic acid, or ethanol and CO_2. This is not a very efficient way of producing energy, for example when compared with eukaryotic respiration, which produces 34 additional *ATP* per molecule of glucose.
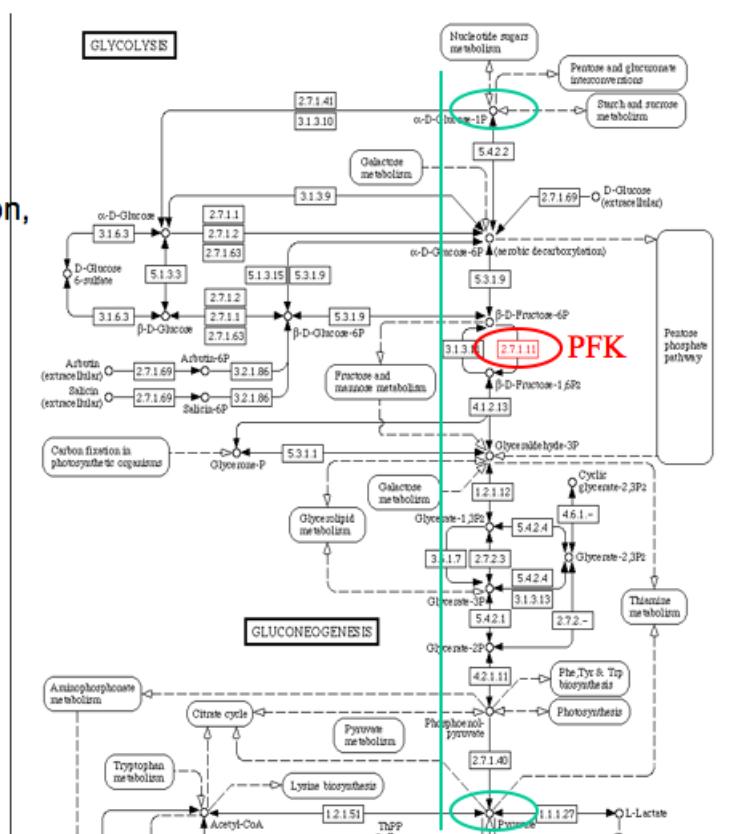
Fig. 5.3. The glycolysis cycle involves the F6P enzyme at the centre of the cascade shown in green.

Reaction modelled (3rd reaction in the chain) :

$$ATP + \text{fructose 6-phosphate} \longrightarrow ADP + \text{fructose 1,6-bisphosphate}$$
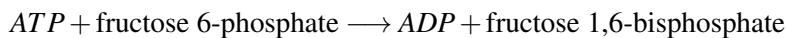
catalysed by the enzyme 6-phosphofructo-kinase (*F6P*); the reaction consumes energy in the form of ATP. In total:

$$ATP + F6P + E \longrightarrow ADP + F1,6BP + E$$
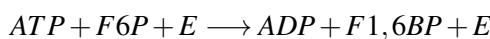
Notation:

- $ATP \equiv y$ (reactant)

- $ADP \equiv x$ (product)

- $Fructose - 6 - phosphatatase(PFK) \equiv E$ (enzyme)

- $Fructose6 - phosphate \equiv F6P$ (reactant)

- $Fructose1,6 - bisphosphate \equiv F1,6BP$ (product)

- the complexes are denoted $(A : B)$

We will consider here the key reactions involving the enzyme E and the molecules ATP/ADP (for more details see the original paper by E.E. Selkov, "Self-Oscillations in Glycolysis", 1968):

- $\emptyset \longrightarrow y$, energy production.

- $2x + E \rightleftharpoons (E : 2x)$, activation of the enzyme by $2ADP$ and formation of the active complex.

- $y + (E : 2x) \rightleftharpoons (y : E : 2x) \rightarrow (E : 2x) + x$, enzymatic reaction according to a Michaellis-Menton mechanism.

- $x \rightarrow \emptyset$, recycling of x.

B. Model. After a second simplification, the enzyme is eliminated (for more details see the original paper by E.E. Selkov, 1968). The model is reduced to:

$$\dot{x} = -x + ay + x^2 y$$
$$\dot{y} = b - ay - x^2 y$$

where x and y represent the concentrations of ADP and ATP, and $a, b > 0$.
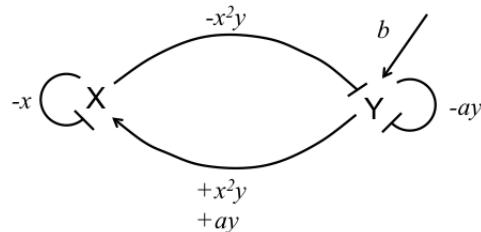
Fig. 5.4. Drawing of the simplified two-component model x and y.

Phase portrait and application of the PBT
A. Isoclines and vector fields

- $\dot{x} = 0$: $y = \frac{x}{a+x^2}$

- $\dot{y} = 0$: $y = \frac{b}{a+x^2}$

Observations. The vector field (Figure 5.5) suggests rotations, are they

- Are they stable or unstable spirals?

- Is there a limit cycle?

The aim is to determine the conditions for a limit cycle, equivalent to oscillations in the ATP/ADP concentrations. We will apply the Poincaré-Bendixon theorem.

B. Construction of the confinement region R.
Consider the region R bounded by five straight lines (Figure 5.5).
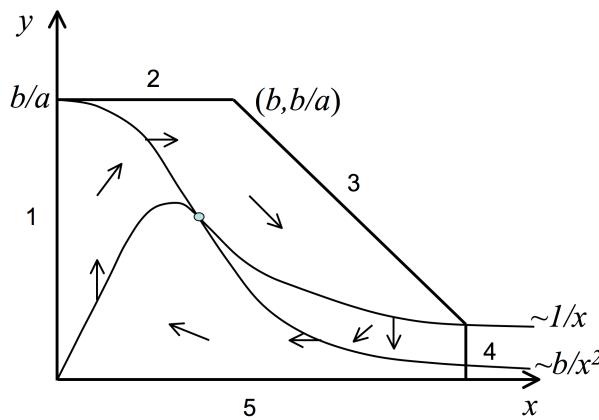
Fig. 5.5. The confinement region for the glycolysis cycle consists of 5 straight lines numbered 1-5. The isoclines are also indicated. The line 3 passes through $(b, b/a)$ with slope -1, so it intersects the isocline $\dot{x} = 0$ as shown, which defines the location of line 4.

To show that R is indeed a confinement region, we must show that the vector field points towards the interior of the region on all portions. Except for the case 3, this follows directly from the orientation of the vector field in the sectors delimited by the isoclines. For the case 3 (line with slope -1), we still have to show that the slope of the vector field is more negative than -1, i.e. $-\dot{y} > \dot{x}$. For this we replace:

$$\dot{x} - (-\dot{y}) = -x + ay + x^2 y + (b - ay - x^2 y) = b - x < 0 \;\; \text{si} \;\; x > b \,, \text{QED} \,.$$

C. Stability of the fixed point
The fixed point is given by $(x^*, y^*) = (b, b/(a+b^2))$ and the Jacobian

$$J(x^*, y^*) = \begin{pmatrix} \frac{b^2-a}{b^2+a} & a+b^2 \\ -\frac{2b^2}{a+b^2} & -(a+b^2) \end{pmatrix}$$

with $\Delta = b^2 + a > 0$ and $\tau = \frac{-(b^4+(2a-1)b^2+a^2+a)}{b^2+a}$. Therefore $\tau > 0$ when the numerator is positive. The limit is given by

$$b^2 = \frac{1-2a \pm \sqrt{1-8a}}{2} \ .$$

The region of existence of a limit cycle is shown in Figure 5.6.
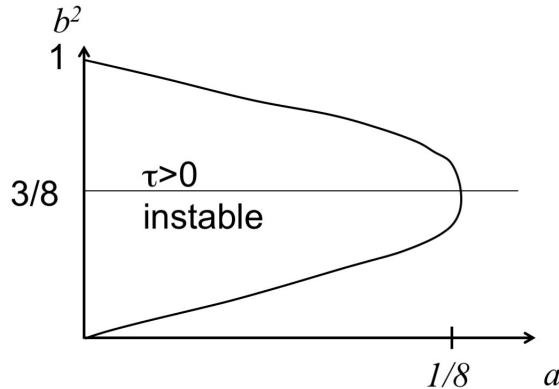
Fig. 5.6. Region of existence of a stable limit cycle in the (a,b) plane. Qualitative representation, the drawing is not to scale.

For a small, $\sqrt{1-8a} \simeq 1-4a$, and therefore

- $b^2 = (1-2a+1-4a)/2 \quad \Rightarrow b^2 = 1-3a$ for the positive branch (sign $+$ in the equation for b^2).

- $b^2 = (1-2a-1+4a)/2 \quad \Rightarrow b^2 = a$ for the negative branch.

- for $a = 1/8 - \varepsilon$, $b^2 = 3/8 \pm \sqrt{2\varepsilon}$.

Conclusion: A limit cycle is found in the confinement region R when a and b are such that $\tau > 0$. A typical phase portrait is shown in Figure 5.7.
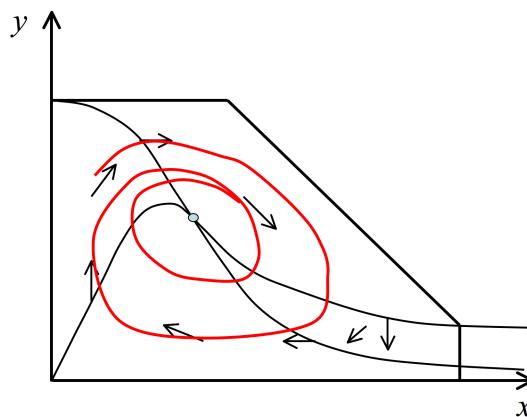
Fig. 5.7. Glycolysis cycle: trajectory approaching the stable limit cycle.

The question arises as to whether the region $\tau > 0$ corresponds to unstable spirals or fixed points. **Hint**: start by analysing the situation for $a = 0$.

5.3 Excitable systems

Systems said *excitables* are closely related to limit cycle oscillators, as it is the case for the Fitz-Hugh Nagumo model studied in the exercises.

6. Entrainment and synchronisation of phase oscillators

There are many situations in which the interactions between oscillators (cellular, neuronal, behavioral) and their environment play an important role. Indeed, these interactions give rise to collective phenomena such as synchronization. For example, the circadian oscillator in humans is driven by daily cycles of light and temperature.

6.1 Forced phase oscillator (sinusoidal coupling)

We study the coupling between an oscillator and its external environment using the following model. An oscillator is subjected to a periodic light stimulus with a period T_e that differs from the intrinsic period T_i of the oscillator.

6.1.1 The model

Hypothesis: The driven oscillator (e.g. the human circadian oscillator) is assumed to be a limit-cycle oscillator, but we're not concerned here with describing the detailed dynamical model that brings these oscillations. Instead, we assume a limit cycle exists and introduce a phase variable.

Parametrization of limit cycles by phase. Let us imagine that the limit cycle is parametrized by a phase $\theta(t)$ and amplitude A (we assume that the amplitude of the cycle is constant), so that the expression of a protein under the control of this oscillator, for example the protein L, can be written as $L(t) = L_0(1 + A\cos(\theta(t)))$.

Furthermore, the stimulus is described as $S(t) = S_0(1 + B\cos(\alpha(t)))$. The aim is to describe the effect of the S cycle on the L cycle.

Phase model

In what follows, we'll consider only phase dynamics. The time dependence of the phase for the cycles takes the form:

$$\dot{\theta} = \omega + K\sin(\alpha - \theta)$$
$$\dot{\alpha} = \Omega \,,$$

where $\omega = 2\pi/T_i$ and $\Omega = 2\pi/T_e$ are the frequency of the oscillator and external stimulus and respectively, and $K\sin(\alpha - \theta)$ defines the coupling of the stimulus on the phase of the circadian oscillator. Note: more generally we would consider a coupling function $f(\alpha - \theta)$ with the only requirement that it is 2π-periodic.

Properties:

- If the oscillator and stimulus are in phase, $\sin(\alpha - \theta) = \sin(0) = 0$.

- If $\theta > \alpha$, then the instantaneous frequency $\dot{\theta}$ is reduced ($\sin(\alpha - \theta) < 0$), and so the coupling tends to align the phases (the θ phase is braked).

- K determines the strength with which the oscillator can change its phase in response to the stimulus.

Model analysis (back to 1D)

To determine whether the oscillator follows the stimulus, which is referred to as entrainment, we define a new variable as the difference between the two phase angles:

$$\varphi = \alpha - \theta$$
$$\Rightarrow \quad \dot{\varphi} = \dot{\alpha} - \dot{\theta} = \Omega - \omega - K\sin(\varphi) \,.$$

Or

$$\frac{d\varphi}{d\tau} = \frac{\Omega - \omega}{K} - \sin(\varphi) \tag{6.1}$$

with $\tau = Kt$. We have thereby reduced the two-dimensional problem to a one-dimensional problem. Let us next put $\mu = \frac{\Omega - \omega}{K}$ and study different cases as the parameter μ is varied:

Case I. $0 < \mu < 1$, where $\mu_c = 1$ is the critical value that delimits the two cases. We find two
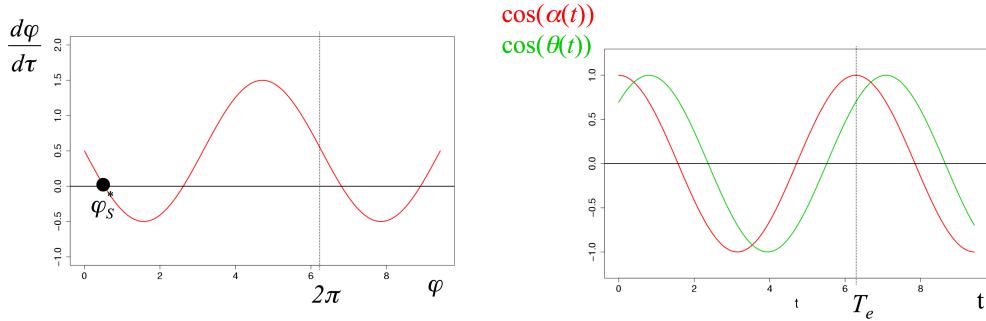
Fig. 6.1. Phase locking (training). Left: Qualitative analysis in 1D; stable FP is shown in bold. Right: Trajectories for long periods of time

.

fixed points, one stable and the other unstable. The phase difference therefore tends towards a constant.

Case II. $\mu > \mu_c$

The fixed points disappear.
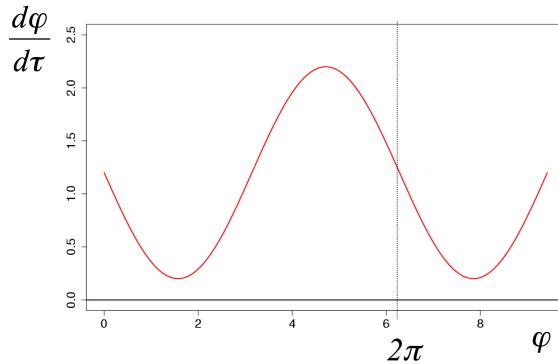
Fig. 6.2. Phase drift. Left: Qualitative analysis in 1D

.

Interpretation: $\varphi(t)$ grows indefinitely, referred to as "phase drift". The frequency difference is too great and the coupling too weak to allow the circadian oscillator to follow the stimulus.

In this regime, it is possible to calculate the drift time, which corresponds to the time required for the φ phase shift to increase by 2π. In other words, it's the time during which the θ phase makes one revolution around the α drive phase:

$$T_d = \int_0^{T_d} dt = \int_0^{2\pi} \frac{dt}{d\varphi} d\varphi = \int_0^{2\pi} \frac{1}{(\Omega - \omega) - K\sin(\varphi)} d\varphi = \frac{2\pi}{\sqrt{(\Omega - \omega)^2 - K^2}} \ ,$$

which is defined for $K < |\Omega - \omega|$ corresponding to the phase drift regime and shows divergence for $K \to |\Omega - \omega|$.

Conclusion

- If $T_e \approx T_i$, the oscillator is driven by the stimulus of period T_e. This is known as "entrainment" or "phase locking". This can occur within a limited interval around its natural frequency.

- If $|T_e - T_i|$ is too large, the oscillator can no longer keep up; this is known as phase drift.

Typically, ω, K are the oscillator's own parameters, while Ω is set by the experimenter.

The main prediction of this model is that the entrainment domain, *i.e.* the frequency of the external stimulus for which entrainment is possible is given by the condition $|\Omega - \omega| < K$.
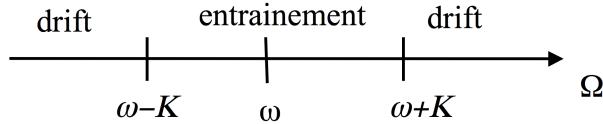
Fig. 6.3. Entrainment interval for Ω when ω and K are fixed.

6.2 Forced phase oscillators (pulsed coupling)

As an alternative model for the coupling between the drive phase and the oscillator, we can consider a more discrete or pulsed coupling than in the previous case (sin coupling). This is a situation in which the coupling only acts for a very brief interval, effectively a pulse that projects the phase to a new value. Consider the following model:

$$\dot{\theta} = \omega + \sum_n \delta(t - nT)g(\theta(t)) \tag{6.2}$$

$$\tag{6.3}$$

$$\text{with} \quad g(\theta) = e \sin(\theta) \, , \tag{6.4}$$

which can also be written as a discrete dynamic system:

$$\theta_{n+1} = F(\theta_n) = \theta_n + \omega T + g(\theta_n) \tag{6.5}$$

where $\theta_n = \theta(nT)$ and we assume that the Dirac delta function δ acts immediately after times $t = nT$. *Note:* in general the function $g(\theta)$ can be any 2π-periodic function. The constant ω is the natural (unforced) frequency of the oscillator, T is the period of the external driving force, and e is the magnitude of the external force.

6.2.1 Fixed points

In a discrete dynamical system, fixed points are defined as follows:

$$\theta^* = F(\theta^*) \, , \tag{6.6}$$

and the task is to find the intersections between the line θ and the function $F(\theta)$ in a representation θ_{n+1} as a function of θ_n.

6.2.2 Case $|e| < T\omega$

In this case, there is no fixed point (Figure 6.4).
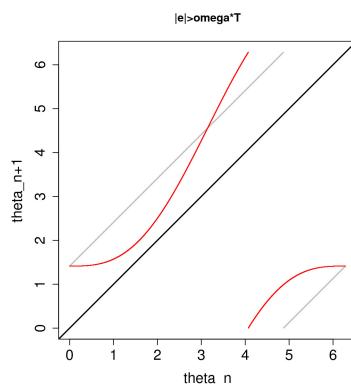
Fig. 6.4. There is no fixed point for the $|e| < T\omega$ case. The $F(\theta)$ function is in red. The orbit is indicated by the vertical black lines

.

6.2.3 Case $|e| > T\omega$

In this case, there is a stable fixed point (Figure 6.5).
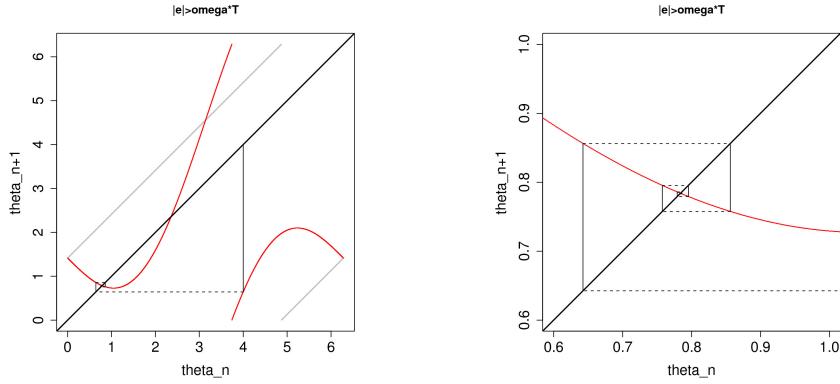
Fig. 6.5. Left: A stable fixed point exists for the case $|e| > T\omega$. Right: Zoom around the fixed point in $\theta \sim 0.8$.

.

6.2.4 Stability criterion for discrete dynamical systems

A discrete SD is stable in θ^* if the sequence $\theta_n - \theta^*$ converges to 0, *i.e.* when

$$\left| \frac{\theta_{n+1} - \theta^*}{\theta_n - \theta^*} \right| \simeq \left| \frac{F'(\theta^*)(\theta_n - \theta^*)}{\theta_n - \theta^*} \right| = \left| F'(\theta^*) \right| < 1 \ . \tag{6.7}$$

Note: here we used that a sequence a_n converges to zero if $\left| \frac{a_{n+1}}{a_n} \right| < 1$. We have also used a Taylor expansion (to first order) for $\theta_{n+1} = F(\theta_n)$ around θ^*.

In (Figure 6.6), we observe a region with a single stable fixed point. Outside $|F'(\theta^*)| < 1$, the dynamics are more complicated, *i.e.* we find

- periodic orbits of period $2T$, $4T$, $8T$, ...

- chaotic orbits

In conclusion, the discrete dynamical system with pulsed coupling shows far more complex dynamics than that with continuous sine coupling.
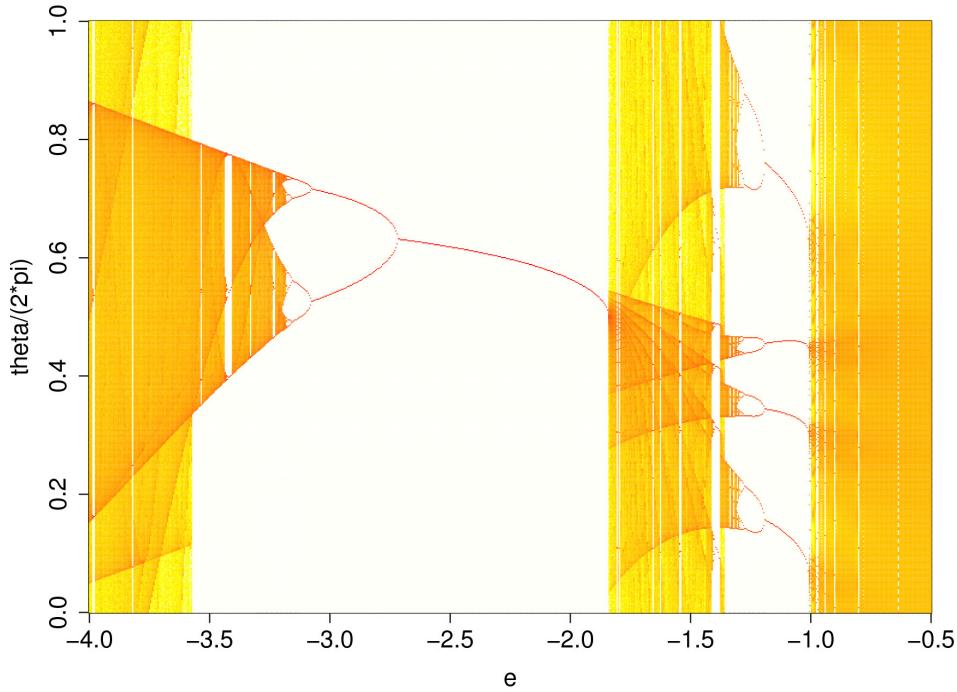
Fig. 6.6. System behavior as a function of coupling e. The range corresponding to the interval $e \in [-2.7, -1.8]$ admits a single stable fixed point (*i.e.* stable orbits with period T, or 1:1 entrainment). For lower e, we find a succession of bifurcations towards orbits with periods of $2^n T$. Colors indicate point density (red: maximum density, white: zero density)

.

6.3 Kuramoto model

The Kuramoto model describes a population of N phase oscillators interacting with each other. It is a generic model for describing collective synchronization. In concrete terms, we consider a large population of N phase oscillators θ_i with natural frequencies ω_i. These frequencies are drawn from a (symmetrical) distribution, *e.g.* for a Gaussian distribution, the probability of an oscillator having a frequency ω is $g(\omega)$, where

$$g(\omega) = \frac{1}{\sqrt{2\pi}\sigma} e^{-\frac{(\omega-\bar{\omega})^2}{2\sigma^2}} \ . \tag{6.8}$$

What's more, these oscillators all interact with each other (all-to-all coupling). There are many variants of the model (frequency distribution, form of coupling, etc), but in its simplest version it takes the following form:

$$\dot{\theta}_i = \omega_i + \frac{K}{N} \sum_{j=1}^{N} \sin(\theta_j - \theta_i), \quad i \in \{1, \ldots, N\} \tag{6.9}$$

This is a dynamic system of dimension N. The question is whether the system is synchronized, *i.e.* whether the coupling K can compensate for the frequency dispersion σ. To do this, we'll consider the $N \to \infty$ case, and introduce the quantity $r \in [0, 1]$ to measure phase coherence in the population:

$$re^{i\Psi} = \frac{1}{N}\sum_j e^{i\theta_j} \, . \tag{6.10}$$

<u>Hypothesis:</u> For $N \to \infty$ and $t \to \infty$, $r(t)$ tends to a constant r and $\Psi(t) = \Psi_0 + \bar{\omega}t$.

The following cases are identified:

- $r = 0$, phases are completely incoherent (no synchronization)

- $0 < r < 1$, phases are partially synchronized

- $r = 1$, phases are identical and therefore maximally synchronous

<u>But:</u> Now we need to determine how r depends on K. To do this, we'll derive a self-consistent equation for r, but first we rewrite the coupling term involving r as follows:

$$re^{i(\Psi - \theta_i)} = \frac{1}{N}\sum_j e^{i(\theta_j - \theta_i)} \tag{6.11}$$

$$\frac{1}{N}\sum_j \sin(\theta_j - \theta_i) = r\sin(\Psi - \theta_i) \, . \tag{6.12}$$

This step is key to the calculation, as it clearly shows the 'mean field' nature of the coupling. In fact, the model is written as

$$\dot{\theta}_i = \omega_i + rK\sin(\Psi - \theta_i), \quad i \in \{1,\ldots,N\} \, ,$$

and so the oscillators are only coupled to each other by the mean phase Ψ, with a reduced coupling rK that depends precisely on phase coherence. This creates a positive feedback phenomenon, as coupling tends to tighten the phases around Ψ, which also increases r.

Without loss of generality, by changing coordinates, we can choose $\bar{\omega} = 0$ and $\Psi_0 = 0$, which brings us back to the following system:

$$\dot{\theta}_i = \omega_i - rK\sin(\theta_i), \quad i \in \{1,\ldots,N\} \quad ,$$

with $g(\omega) = g(-\omega)$ a symmetrical distribution in zero. Note the similarity with Equation 6.1!

This analogy allows us to identify two populations of oscillators: the first, entrained by the mean field, with $|\omega| < Kr$, and the other with $|\omega| > Kr$, which corresponds to drifting oscillators. For the former, the stationary phase of each oscillator depends on its frequency according to the implicit equation

$$\omega_i = rK\sin(\theta_i) \, . \tag{6.13}$$

For the second population, we can introduce a stationary phase distribution for each frequency

$$\rho(\theta|\omega) = \frac{C}{v(\theta,\omega)} \, ,$$

with $v(\theta,\omega) = |\omega - rK\sin(\theta)|$ the instantaneous angular velocity and the normalization constant C such that $\int d\theta \rho(\theta|\omega) = 1$. To understand this expression we can think that the time that an oscillator spends in state $s = \theta$ is inversely proportional to its velocity.

Note: This result follows from the continuity equation for phase density (conservation of total density), *i.e.*

$$\frac{\partial}{\partial t}\rho + \frac{\partial}{\partial \theta}(v(\theta)\rho) = 0 .$$

So we see that $\rho(\theta + \pi|\omega) = \rho(\theta|-\omega)$, an important symmetry property for what follows.

We can now calculate r as

$$r = \langle e^{i\theta}\rangle_s + \langle e^{i\theta}\rangle_d$$

where $\langle \cdot \rangle_s$ represents the average over the synchronized population, and $\langle \cdot \rangle_d$ that over the phase-drifted population.

It follows that

$$\langle e^{i\theta}\rangle_s = \langle \cos(\theta)\rangle_s = \int_{-Kr}^{Kr} \cos(\theta(\omega))g(\omega)d\omega ,$$

because $\langle \sin(\theta)\rangle_s = 0$ since the function $\sin(\theta(\omega))$ is odd in ω.

Let's start with the drifting population, where

$$\langle e^{i\theta}\rangle_d = \int_{-\pi}^{\pi} d\theta \int_{|\omega|>Kr} d\omega \, e^{i\theta}\rho(\theta|\omega)g(\omega) = 0$$

by virtue of the symmetry properties $\rho(\theta + \pi|\omega) = \rho(\theta|-\omega)$ and $g(\omega) = g(-\omega)$. The calculation can be done as follows: i) separate the integral into ω in its positive and negative parts; ii) for one of the two terms change $\theta \to \theta + \pi$; iii) use the fact that $e^{i\theta} + e^{i(\theta+\pi)} = 0$.

By changing the variable ($\omega \to \theta$ using Equation 6.13), we find

$$r = \langle \cos(\theta)\rangle_s = rK \int_{-\pi/2}^{\pi/2} \cos^2(\theta)g(Kr\sin(\theta))d\theta , \tag{6.14}$$

the self-consistent relation for r we're looking for, which provides an implicit relationship between r and K.

This relation comprises two branches $r(K)$, the first $r = 0$, and a second more complicated one. However, we can see (by simplifying by r in Equation(6.14)) that this second branch passes through

$$K_c = \frac{2}{\pi}\frac{1}{g(0)}$$

at $r = 0$.

Although you can go further by calculation, it's easiest to calculate the function numerically. See the accompanying Jupyter Notebook.

The result is shown in Figure 6.7. The system is completely unsynchronized for $K < K_c$ or the $r = 0$ branch corresponding to a uniform phase distribution is stable. For $K > K_c$, the system develops partial synchronization, with square-root behaviour. Moreover, for $K > K_c$, the $r = 0$ branch is unstable. Note that the stability properties of the branches cannot be easily derived and require deeper analysis. However, simulations allows us to easily assess the stability of the solutions.

In conclusion, it is remarkable that in this complicated system, it is possible to calculate the critical coupling value K_c needed to synchronize a population of $N \to \infty$ oscillators in a relatively simple way. This is a consequence of the 'mean field' nature of the model.
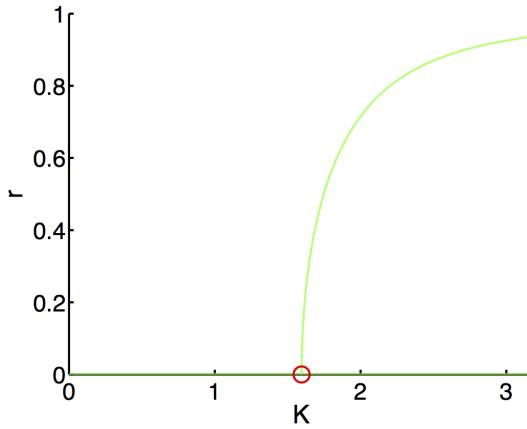
Fig. 6.7. Synchronization in the Kuramoto model. The two branches are shown in green, and the red dot corresponds to $(K_c, 0)$.

.

6.3.1 Explicit solution for the Cauchy distribution

When the frequency distribution is the Cauchy distribution

$$g(\omega) = \frac{1}{\pi} \frac{\gamma}{(\gamma^2 + \omega^2)} \ , \tag{6.15}$$

it is possible to use the definite integral

$$\int_{-\frac{\pi}{2}}^{\frac{\pi}{2}} \cos^2\theta \, \frac{\gamma}{\pi \left(\gamma^2 + (Kr\sin\theta)^2 \right)} d\theta =$$

$$\int_{-\frac{\pi}{2}}^{\frac{\pi}{2}} D \frac{\cos^2\theta}{\left(1 + A\sin^2\theta\right)} d\theta =$$

$$\frac{D}{A} \pi \left(\sqrt{A+1} - 1 \right) \ ,$$

with

$$A = \frac{K^2 r^2}{\gamma^2} \quad \text{et} \quad D = \frac{1}{\pi\gamma}.$$

After a few algebraic transformations, we obtain an explicit expression for the non-trivial branch $r(K)$ for $K \geq K_c$, namely

$$1 = r^2 + 2\frac{\gamma}{K}$$

$$\Leftrightarrow \tag{6.16}$$

$$r = \sqrt{1 - \frac{K_c}{K}} \ ,$$

with $K_c = 2\gamma$.

7. Bifurcations in one and two dimensions

The time evolution of a dynamical system in one dimension (1D) is completely determined by the location and type of its fixed points: the trajectories are monotonic, and either approach a fixed point or move away to infinity. Dynamical systems in 2D or higher exhibit more complex dynamics, but the trajectories of a system are still determined by the location and type of its fixed points.

In many cases the location and/or stability of a fixed point depends on one or more parameters, and the system's behaviour can change dramatically for a small change in the parameters. If there is a *qualitative* change in the dynamics of a system as a parameter passes through a particular value, we say that a *bifurcation* has occurred. There are many types of bifurcation, but in this chapter we consider local bifurcations, which depend only on the state of trajectories close to the fixed point. We do not discuss global bifurcations, but refer the reader to Strogatz.

We first classify the ways that a fixed point of a 1D dynamical system may respond to changes in a parameter. This is not so limiting as it might at first appear. In higher dimensions, the dynamics at a bifurcation often reduce to a 1D problem because motion in the other dimensions simply approaches the 1D manifold on which the bifurcation occurs. Next, we extend our study to 2D systems, and study the higher-dimensional analogues of the 1D bifurcations. We conclude with a detailed examination of the experimentally important, and potentially dangerous, change of a system's dynamics that occurs at the so-called Hopf bifurcation.

7.1 Bifurcations in 1D

Definition 7.1.1 A bifurcation occurs when there is a qualitative change in the dynamics of a system as a parameter is varied, e.g., the appearance or disappearance of a fixed point, or a change in its stability. The dynamics of the system splits into different types on passing through the bifurcation point. Parameters that cause such changes are often referred to as control parameters, as they can be used to vary the behaviour of the model.

Consider the generic form of an autonomous, one-dimensional ordinary differential equation (ODE) that depends on a real parameter r:

$$\frac{dx}{dt} = F(x(t), r) \quad , \quad x, r \in \mathbb{R} \tag{7.1}$$

There are several forms of bifurcation in such a system, and we examine each of them in turn.

7.1.1 Saddlenode bifurcation

A saddlenode bifurcation is the main mechanism by which fixed points appear and disappear in a dynamical system as a control parameter is varied. Other names for a saddlenode are fold bifurcation, turning point bifurcation, and blue sky bifurcation. The latter refers to the appearance of the two fixed points above the bifurcation point out of the "clear blue sky." Note that fixed points are always created in pairs at a saddlenode bifurcation (why?).

The standard form of a saddlenode bifurcation is the following:

$$\frac{dx}{dt} = r - x^2 \tag{7.2}$$

In this equation, the real constant r is the control parameter. For negative values of r, there are no fixed points in the system. When r passes through zero to positive values, a stable and an unstable fixed point are created whose location depend on the magnitude of r. Exactly at the critical value (r = 0, here), a semi-stable fixed point exists, which splits into the two fixed points when r becomes positive.

The vector field (referred to as Graph 1 in Section 1.3) corresponding to the cases of $r < 0$, $r = 0$, and $r > 0$ is shown in Figure 7.1 below. The type of the fixed points is shown by a solid dot for stable ones, and a hollow dot for unstable ones. Semi-stable fixed points are half filled dots, with the filled half on the side which is stable. Although the name saddlenode bifurcation does not make much sense in 1D, in 2D it refers to the property that the node is stable when approached in one direction but unstable in another direction, similar to the shape of a saddle on a horse.
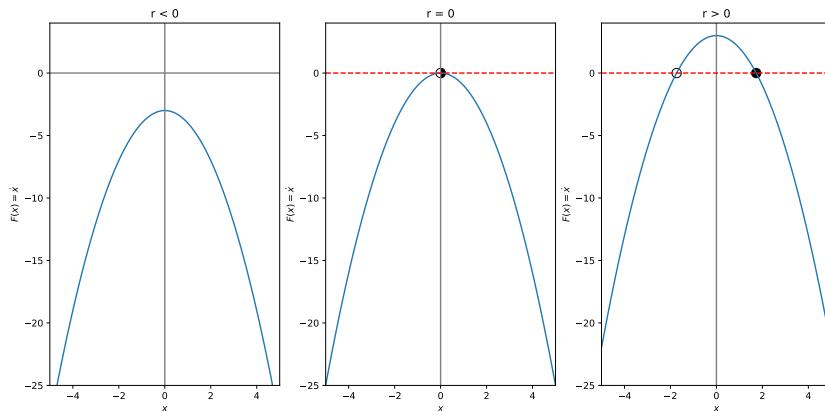
Fig. 7.1. dx/dt versus x for the prototypical saddlenode bifurcation. Above the critical parameter value, r = 0, a stable and unstable node appear. Conversely, the two fixed points present above the critical value of r approach each other and annihilate at the critical value r = 0.

The locations of the fixed points in Figure 7.1 clearly depend on the parameter *r*. It is useful to display this dependence in a graph, which is referred to as a *bifurcation diagram*. To do this we plot the location of the fixed point(s) x^* on the ordinate against the control parameter *r* on the abscissa. Figure 7.2 shows this dependence for the saddlenode bifurcation. Solid curves denote a branch of stable fixed points, and dashed curves denote a branch of unstable ones. If there are no fixed points in a range (as for the saddlenode diagram for r < 0), no curve is drawn.

Note that for convenience and clarity, we often choose dynamical equations for which the critical value of the control parameter is zero. But this is not necessary. Any real value may define a bifurcation in the system.
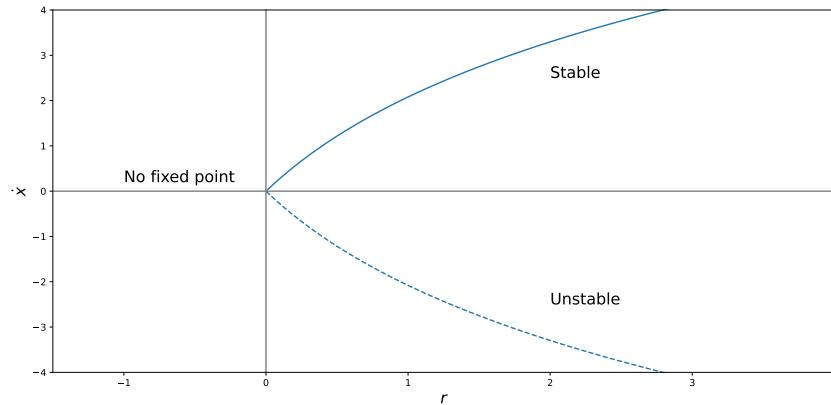
**Fig. 7.2.** Bifurcation diagram for the prototypical saddlenode bifurcation. Above the critical parameter value $r = 0$, a stable and unstable node appear, and move apart as r increases. From Equation 7.2, it can be seen that the two fixed points occur at $\pm\sqrt{r}$.

7.1.2 Transcritical bifurcation

In some cases, a fixed point must occur for all values of a control parameter r. An example is the population models of Section 1.4. The dynamical equation often takes the form:

$$\frac{dN}{dt} = Nf(N, r) \tag{7.3}$$

where N is the size of the population, and r is a control parameter. The presence of the N ensures that the point $N = 0$ is always a fixed point. This is plausible because if there are no individuals in a population, no reproduction occurs. Obviously, this would not be suitable for populations in which spontaneous generation, or migration of new individuals, were to take place.

Although the fixed point at $N = 0$ does not move, it may change its stability as the parameter r varies. The standard equation for this behaviour is the transcritical bifurcation (trans = latin for *across* or *through*):

$$\frac{dx}{dt} = rx - x^2 \tag{7.4}$$

In this scenario, except for the critical value, there are always two fixed points, one of which is always at the origin. Figure 7.3 shows how the fixed point at $x^* = 0$ changes its stability from stable ($r < 0$) to unstable ($r > 0$), while the other fixed point changes in the opposite manner from unstable ($r < 0$) to stable ($r > 0$).

Note that the name only applies to the fixed point whose location is constant but which changes stability. The presence or absence of other fixed points does not affect the labelling of the one under consideration. The bifurcation diagram for a transcritical bifurcation is shown in Figure 7.4. Note that the non-zero fixed point changes its stability but its location also changes, it does not therefore undergo a transcritical bifurcation.

7.1.3 Pitchfork bifurcation

A third type of bifurcation occurs in systems that possess a certain symmetry, such as left-right spatial symmetry (i.e., the equation of motion remains unchanged if x is everywhere replaced by
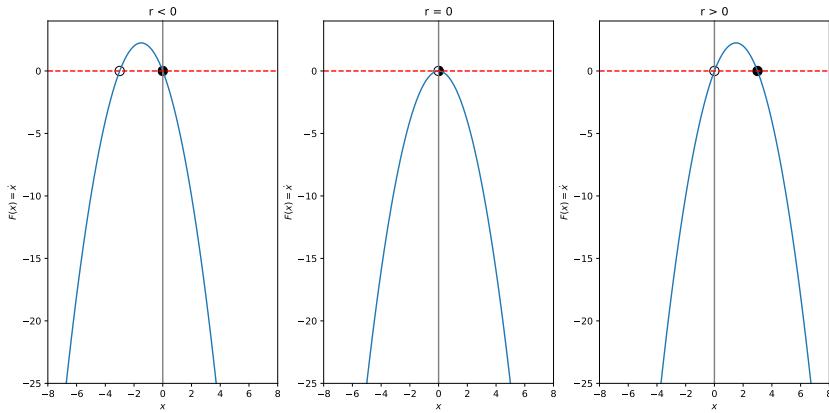
Fig. 7.3. Transcritical bifurcation stability change for the fixed point at the origin.
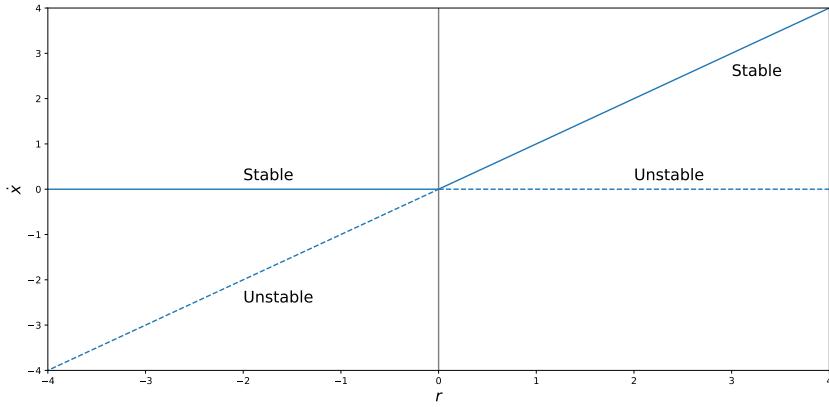
Fig. 7.4. Bifurcation diagram for the prototypical transcritical bifurcation at the origin. As the parameter r increases from negative to positive, the fixed point at the origin loses stability, and becomes unstable.

$-x$). This is the most complex, and therefore most interesting, type of bifurcation in 1D. Unlike the previous cases, this type of bifurcation comes in two varieties — supercritical and subcritical — which exhibit very different dynamics when the critical point is traversed. The second one is responsible for dangerous transitions in real-world engineering scenarios, such as the collapse of the Tacoma Narrows bridge in the USA in 1940.

Supercritical pitchfork bifurcation

We start with the simpler case, in which a single stable fixed point at the origin becomes unstable and two stable fixed points appear as the control parameter increases through the critical value. Note that the origin of the name supercritical lies in the existence of the non-zero fixed points being *above* the bifurcation point.

The canonical equation for this type of bifurcation is:

$$\frac{dx}{dt} = rx - x^3 \tag{7.5}$$

It is clear that this equation has three fixed points when $r > 0$, located at $x^* = 0$, and $x^* = \mp\sqrt{r}$,

but only the origin is a fixed point for $r < 0$. The vector field for this case is shown in Figure 7.5 below.
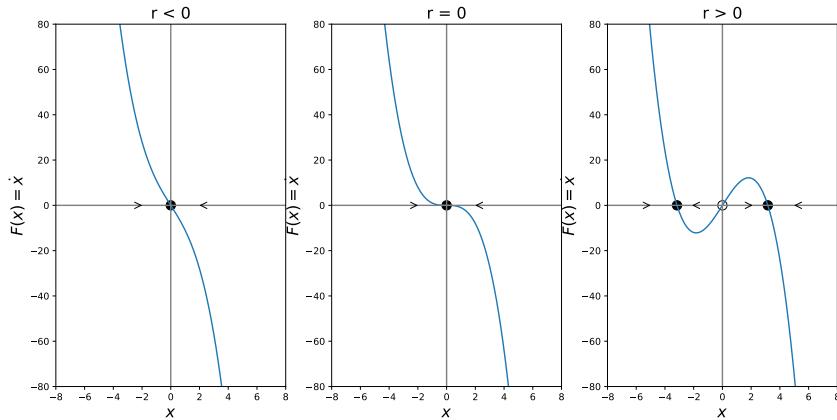
Fig. 7.5. dx/dt versus x for the prototypical supercritical pitchfork bifurcation. Note that the distance of the non-zero fixed points from the origin increases continuously with the paramer μ above the bifurcation. This explains why it is referred to as a soft, safe, or continuous bifurcation.

The bifurcation diagram for a supercritical pitchfork bifurcation is shown in Figure 7.6. It reveals the following interesting behaviour. Consider a system with control parameter $r < 0$. All trajectories are attracted to the single stable fixed point at the origin. But when the parameter is positive, the origin becomes unstable, and the system will follow a trajectory to one of the stable branches of fixed points, the locations of which depend on the value of the control parameter.
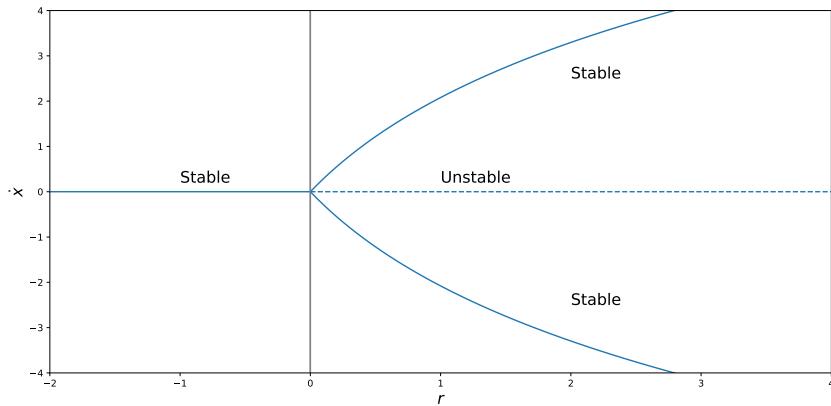

Fig. 7.6. Bifurcation diagram for the prototypical supercritical bifurcation. Above the critical parameter value r = 0, the fixed point at the origin becomes unstable, and two stable fixed points appear and move apart as the control parameter increases. From Equation 7.5, it can be seen that the two non-zero fixed points occur at $\pm\sqrt{r}$.

Importantly, the locations of the stable fixed points increases continuously from zero, proportional to $\sqrt{r}$, when $r > 0$. This implies that just above the bifurcation point there is no jump in the location of the fixed point. Figure 7.6 also reveals the origin of the name in the shape of the branches of the fixed points above the bifurcation.

The slow, continuous movement of the stable branches of fixed points away from the origin in

the supercritical pitchfork bifurcation is in sharp contrast to the subcritical pitchfork bifurcation, to which we turn next.

Subcritical pitchfork bifurcation

The canonical equation for a subcritical pitchfork bifurcation is:

$$\frac{dx}{dt} = rx + x^3 \tag{7.6}$$

It is useful to compare this case with the previous supercritical case described by equation 7.5. Whereas the (negative) cubic term in that case stabilised the system (by pulling trajectories back to the origin), the (positive) cubic term in equation 7.6 *destabilises* it. When the control parameter is above the critical value, there are no stable fixed points to attract the system (see Figure 7.7). It is the absence of other fixed points that makes this type of bifurcation dangerous, because a small change in the control parameter near the critical point results in unbounded excursions of the system away from the previously stable fixed point at the origin.

Figure 7.7 shows that in a subcritical pitchfork bifurcation ,there is a stable fixed point at the origin brackets between two non-zero branches of unstable fixed points when the control parameter is below the critical value, which here is $r = 0$. When the parameter increases through the bifurcation point, the origin becomes unstable and the non-zero fixed points vanish. Because the non-zero fixed points only occur for values of the control parameter *below* the critical value, it is referred to as *subcritical*.

The fixed points for this system are shown in Figure 7.7.
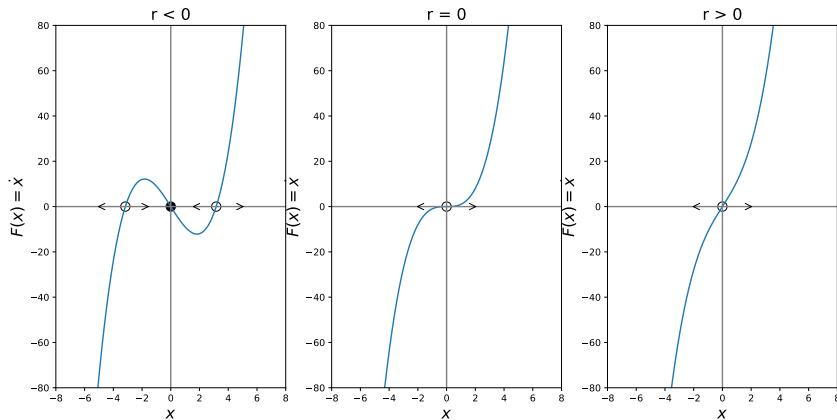
Fig. 7.7. dx/dt versus x for the subcritical pitchfork bifurcation. Unlike the supercritical case in Figure 7.5, there are no stable fixed points above the bifurcation point, and trajectories will flow away to infinity unless additional terms are included in the original dynamic system equations. It is therefore referred to as a hard, discontinuous, or dangerous bifurcation.

The bifurcation diagram for a system undergoing a subcritical pitchfork bifurcation is shown in Figure 7.8 below. This also reveals that even below the bifurcation point, sufficiently large perturbations could drive the system beyond the bracketing unstable fixed points, which would result in the system moving along a trajectory towards infinity. This becomes increasingly possible as the system approaches the bifurcation point (from below).

Consider what happens to a system initially located at its stable fixed point for $r < 0$ as r is increased through the critical point. At first, any small perturbation to the system (where small means that it does not take the system beyond the unstable non-zero fixed points) decays to zero,
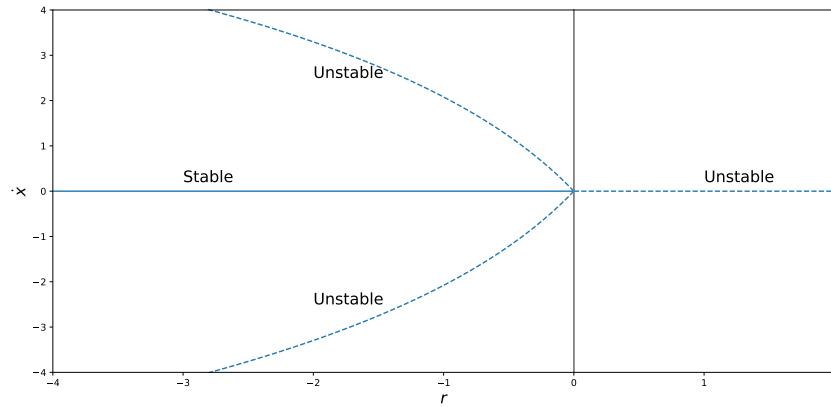
Fig. 7.8. Bifurcation diagram for a subcritical pitchfork bifurcation. Above the critical value of control parameter there are no stable fixed points, and the system will follow a trajectory to infinity. From Equation 7.6, it can be seen that the two non-zero fixed points below the bifurcation occur at $\pm\sqrt{|r|}$.

and the system is stable against such disturbances. But when the control parameter is positive, the stable fixed point disappears, and a small perturbation to the system will grow, and the system diverges to infinity. In engineering problems (e.g., increasing vibration of aircraft wings as the speed increases), a system that passes through a subcritical pitchfork bifurcation can exhibit the unbounded growth of small perturbations unless some other influence is present to dampen them.

In physical situations, the instability is often opposed by additional damping mechanisms. These are represented in the equation by higher-order terms. In order to preserve the symmetry, the first term that can appear is a fifth power in the variable x:

$$\frac{dx}{dt} = rx + x^3 - x^5 \tag{7.7}$$

The bifurcation diagram for a system undergoing a subcritical pitchfork bifurcation with the stabilising fifth power is shown in Figure 7.9 below. It exhibits the phenomenon called hysteresis (discussed earlier in the 1D model for the bistable chemical switch described in chapter 2.)

When the control parameter increases from a negative value, the system stays at the stable fixed point at $x^* = 0$ until the parameter becomes positive. Then, the origin becomes unstable, and the system jumps to a fixed point on the stable branch at a finite value of x^*. Additionally, if the control parameter is subsequently reduced below zero, the system does not return to the stable fixed point at $r = 0$, but only at a lower value, which for this model occurs at $r = -1/4$. This implies that once the system has jumped to the distant stable fixed point, it can only be restored to stability by reducing the control parameter below the original value at the bifurcation point.
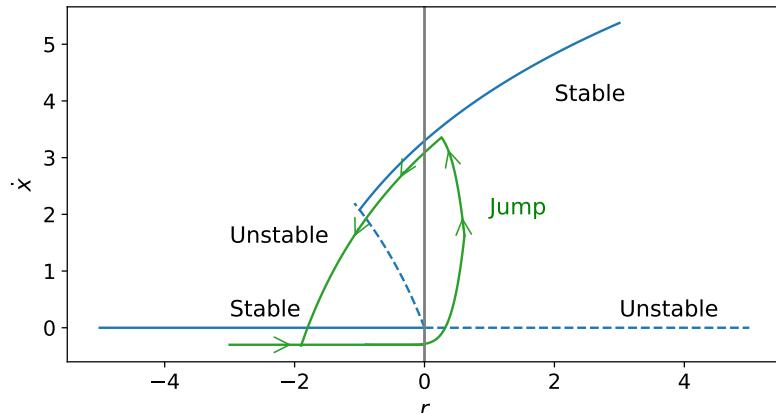
Fig. 7.9. Bifurcation diagram for a subcritical pitchfork bifurcation with a stabilising $-x^5$ term. The green curve shows how a system initially at the stable fixed point $x^* = 0$ behaves as the control parameter r is increased above the bifurcation value and then reduced below it. Above the critical value, $r = 0$, the system jumps to a distant fixed point on the stable branch, and remains there even when the control parameter is reduced to the value at the bifurcation point. A further reduction of the parameter is needed to restore the system to its original stable state. This is the phenomenon of hysteresis.

7.2 Bifurcations in 2D

Two dimensional dynamical systems also exhibit bifurcations, but in general the qualitative changes in the fixed points take place in a 1D subspace, while dynamics in the orthogonal space is simple attraction or repulsion from the first subspace. We know from Chapter 3 that trajectories in 2D dynamical systems have more possibilities for their long-time behaviour than those of 1D systems. These include the oscillatory solutions of centres, spirals, and limit cycles (see Chapter 5. Just as fixed points in 1D systems can move or change stability as a parameter is varied, so too can these 2D fixed points undergo bifurcations.

7.2.1 Simple 2D bifurcation

Suppose a given 2D dynamical system has a stable fixed point for a certain parameter value, μ. In which ways can this fixed point change its stability? By assumption that it is stable, the eigenvalues of the Jacobian at the fixed point must either be both real and negative or complex conjugates with a negative real part. In the former case, if one of the eigvenvalues becomes positive as the parameter changes, the fixed point undergoes a saddlenode, transcritical or pitchfork bifurcation, and can be studied using the methods of Section 7.1. If, however, the real part of a pair of complex conjugate eigenvalues crosses the imaginary axis and become positive, a new form of bifurcation occurs: the Hopf bifurcation.

First, we consider a saddlenode bifurcation in a 2D system. A simple example is given by the following equations:

$$\frac{dx}{dt} = \mu - x^2 \tag{7.8}$$

$$\frac{dy}{dt} = -y \tag{7.9}$$

This system is particularly simple because the two equations are decoupled. The motion in

the Y dimension is exponentially damped towards the X axis, while along the X axis, there is a saddlenode bifurcation at the parameter value $\mu = 0$.

The phase portraits for this system for $\mu > 0$, $\mu = 0$, and $\mu < 0$ are shown below in Figure 7.10. NB Note the reversed order of the values of μ.
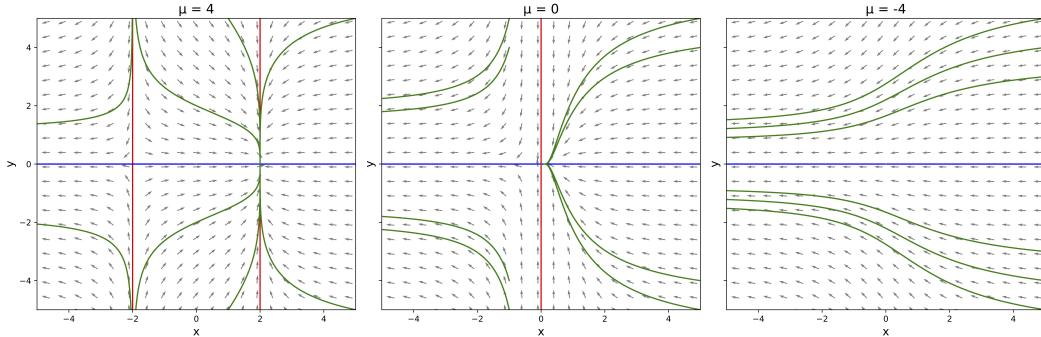

Fig. 7.10. dx/dt versus x for the prototypical 2D saddlenode bifurcation. Below the critical parameter value, $\mu < 0$, there are no fixed points. At the critical value, $\mu = 0$, a semi-stable fixed point appears at $x^* = 0$, and above the critical value, $\mu > 0$, there are two fixed points: a stable node at $x^* = \sqrt{(\mu)}$ and a saddlepoint at $x^* = -\sqrt{(\mu)}$.

When $\mu > 0$, there is a stable node at $x^* = \sqrt{\mu}$, and a saddlepoint at $x^* = -\sqrt{\mu}$. Linearising the Jacobian around the fixed points allows one to obtain the fast and slow eigenvectors of the stable node and the stable and unstable manifolds of the saddlepoint. Note that the direction of approach of trajectories to the stable node depends on the magnitude of the parameter μ. This can be seen by finding the eigenvalues and eigenvectors of the Jacobian matrix, which are -1 (Y axis) and $-2\sqrt{\mu}$ (X axis). If $2\sqrt{\mu} < 1$, then the slow direction is the X axis, which is the case shown in the figure, but if $2\sqrt{\mu} > 1$, the slow direction is the Y axis.

When $\mu = 0$, Equations 7.8, 7.9 show that there is a fixed point at the origin (0, 0). Trajectories originating in the positive X half plane flow to this fixed point. But trajectories that originate in the left X half plane flow to minus infinity along the X axis: the origin is therefore a semi-stable node. However, if one attempts to find the fast and slow eigenvectors for this node, the fast eigenvector is easily found to be the Y axis, but the procedure fails to find the slow eigenvector along the X axis. Consideration of the original equations shows that this is because the linearisation about the fixed point, which is needed to obtain the Jacobian, fails. Higher order terms, namely $-x^2$ control the flow at the fixed point.

Similar reasoning about the fast and slow eigenvectors discussed earlier applies to trajectories that approach the semi-stable node at $x^* = 0$ when $\mu = 0$.

It is apparent from the vector field that when $\mu < 0$ there are no fixed points; all trajectories head off to minus infinity, asymptotically parallel to the X axis. However, there is a "ghost" region around the location of the vanished fixed point at $x^* = 0$. Motion of the system through this region motion is dramatically slowed down. This arises from the nonlinear term in the x equation, which has the effect that the magnitude of the dx/dt term drops quadratically when $x < 1$. Alternatively, one can see this by noting that the gradient is large when x is larger than one, but as x approaches zero (where the fixed point used to be), its magnitude drops quadratically, so the system takes longer to traverse the region around the missing fixed point.

7.2.2 Genetic control system as a 2D bifurcation model

Consider the following model for translation of mRNA into its associated protein:

$$\frac{dx}{dt} = -ax + y \tag{7.10}$$

$$\frac{dy}{dt} = -by + \frac{x^2}{1+x^2} \tag{7.11}$$

where we take x = [Protein] and y = [mRNA], and the two parameters a and b are positive real constants. This can be compared to the model for a bistable chemical switch that we examined in Chapter 2. Whereas in that 1D model, only the concentration of protein was explicitly represented in the equations, we now include the dynamics of both the protein and the mRNA. This allows us to capture more sophisticated behaviour, including the qualitative change in the dynamics as the parameters a, b are changed.

First, we identify the terms that occur in the equations. The linear terms $-ax$ and $-by$ represent time-dependent removal, or degradation, of the protein and mRNA respectively. The y term in the first equation corresponds to the production of protein from the messenger RNA, and the $x^2/(1+x^2)$ term in the second equation represents the saturating positive feedback of the protein on its own translation from the RNA.

The nullclines are obtained from the conditions $dx/dt = 0$, and $dy/dt = 0$, and are respectively:

$$y = ax \tag{7.12}$$

$$by = \frac{x^2}{1+x^2} \tag{7.13}$$

The X nullcline is a straight line with a slope given by the protein degradation parameter a. The Y nullcline is an S-shaped curve, which asymptotically approaches the value $1/b$ at large x. Figure 7.11 shows the nullclines for three values of the parameter a —small, intermediate, and large.

We now consider what happens to the dynamics of the system if the RNA decay parameter b is fixed, and we allow that of the protein a to vary. Fixed points of the system occur at the intersections of the nullclines, and we see from Figure 7.11, that the origin is the only fixed point for large values of the parameter a. In this case, the protein degrades too quickly to support its own production. However, as the parameter a is reduced, it reaches a critical value $a = a_c$ at which the two nullclines become tangent to each other, and a second fixed point appears. Further reduction of a results in a third fixed point appearing at a large value of protein concentration. As a represents the degradation rate of the protein, we see that a high rate of decay results in the protein disappearing, while a low decay rate allows a high concentration of protein to build up. The third fixed point (between these two) controls how these two stable states are separated.

Eliminating the variable y between Equations 7.12 and 7.13 allows us to determine the location of the fixed points, which gives, after eliminating $x^* = 0$

$$ab((1+x^2) = x. \tag{7.14}$$

The two roots of this equation are easily found to be:

$$x_1^* = \frac{1}{2ab}[1 - (1 - (2ab)^2)^{1/2}] \tag{7.15}$$

and

$$x_2^* = \frac{1}{2ab}[1 + (1 - (2ab)^2)^{1/2}]. \tag{7.16}$$

From these equations we can see that if $2ab > 1$, the only fixed point of the system is at $x^* = 0$; when $2ab = 1$, an additional fixed point occurs at $x^* = 1$; and, finally, if $2ab < 1$, there are two real roots x_1^*, x_2^* in addition to $x = 0$:

We can find the critical parameter value a_c at which the nullclines become tangent (considered as a function of the parameter b) from the two conditions: 1) the function values are equal, and 2) the tangents of the functions are equal. This gives us the following condition:

$$ab = \frac{x}{1 + x^2} \tag{7.17}$$

and (from the equal tangents):

$$ab = \frac{2x}{(1 + x^2)^2} \tag{7.18}$$

Dividing Equation 7.17 by Equation 7.18 shows that the tangent condition, defined by $2a_c b = 1$, occurs at $x^* = 1$.

We obtain the types of the fixed points from the Jacobian of the system:
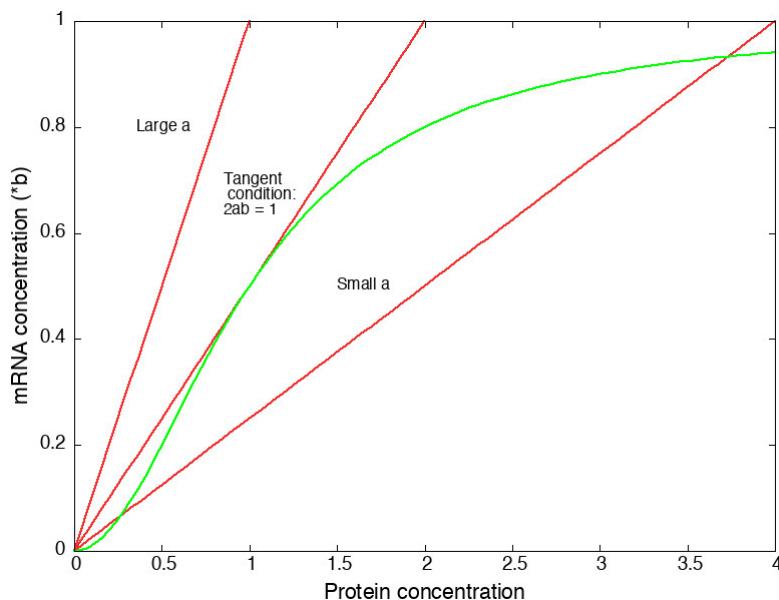

Fig. 7.11. Nullclines for the genetic control system for a fixed value of the parameter b, and small, intermediate, and large values of the parameter a. A fourth line is drawn for the particular value of a at which the two nullclines are tangent to each other, which occurs at the point $x^* = 1$.

$$J = \begin{pmatrix} -a & 1 \\ \frac{2x}{(1+x^2)^2} & -b \end{pmatrix}$$

with trace and determinant:

$$\tau = -(a+b) \qquad\qquad \Delta = ab - \frac{2x}{(1+x^2)^2}$$

Because the trace is negative (recall that $a, b > 0$), all fixed points must either be stable nodes or spirals, or saddlepoints. Let us now examine each fixed point in turn.

A) $(x^*, y^*) = (0,0)$

At the origin, the Jacobian is:

$$J = \begin{pmatrix} -a & 1 \\ 0 & -b \end{pmatrix}$$

with trace and determinant:

$$\tau = -(a+b) \qquad\qquad \Delta = ab$$

from which we find,

$$\tau^* - 4\Delta = (a-b)^2 > 0. \tag{7.19}$$

and the origin is therefore a stable node for all values of a, b.

B) $x_1^* = \frac{1}{2ab}[1 - (1 - (2ab)^2)^{1/2}]$

We know that $\tau = -(a+b) < 0$, but what is Δ? From above

$$\Delta = ab - \frac{2x_1^*}{(1 + (x_1^*)^2)^2} \tag{7.20}$$

and although this looks hard to solve, given the expression for x_1^*, we know that Equation 7.17 holds at the fixed point, and therefore we find

$$\Delta = ab\frac{((x_1^*)^2 - 1)}{(1 + (x_1^*)^2)}. \tag{7.21}$$

Further, given that $x_1^* < 1$ (why?), we see that $\Delta < 0$, and this fixed point must be a saddlepoint.

C) $x^* = \frac{1}{2ab}[1 + (1 - (2ab)^2)^{1/2}]$

As in case B), we know that $\tau < 0$, and try to find Δ again from:

$$\Delta = ab - \frac{2x_2^*}{(1 + (x_2^*)^2)^2}. \tag{7.22}$$

We use the same substitution as in Case B) to get

$$\Delta = ab\frac{((x_2^*)^2 - 1)}{(1 + (x_2^*)^2)}, \tag{7.23}$$

but this time we know that $x_2^* > 1$ (why?), so the numerator is positive and smaller than the denominator. Therefore, $0 < \Delta < ab$, which means that $\tau^2 - 4\Delta > (a-b)^2 > 0$. This fixed point is therefore a stable node.
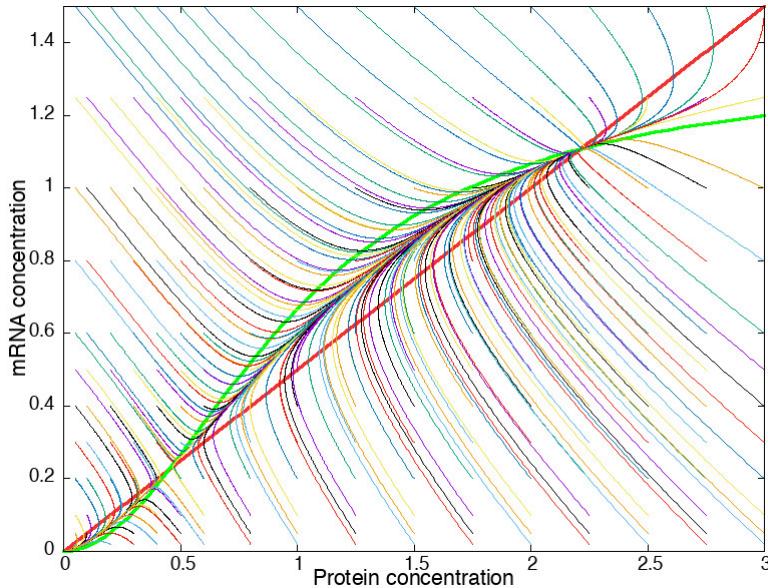

Fig. 7.12. Phase portrait for the Genetic Control System with the parameter values $a = 0.5, b = 0.75$. Three fixed points occur at $(0,0)$, $\sim (0.45, 0.225)$ and $\sim (2.215, 1.11)$, and are, respectively, a stable node, a saddlepoint, and a stable node. The thick red and green curves show the X and Y nullclines according to Equations 7.12 and 7.13 respectively.

Figure 7.12 shows the phase portrait for the case $a = 0.5, b = 0.75$, which satisfies the condition $2ab < 1$, and has three fixed points. The stable nodes at $(0,0)$ and (approximately) $(2.215, 1.11)$ are separated by the saddlepoint at (again, approximately) $(0.45, 0.225)$. We see from the figure that the phase plane is divided into two distinct regions, separated by the stable manifold of the saddlepoint. Trajectories on either side of this manifold eventually approach one or other of the two stable nodes. The stable manifold is a *separatrix*, and forms a boundary between regions of the phase plane whose trajectories have very different long-time dynamics.

This system exhibits bistability (as did the 1D bistable chemical switch in Chapter 2); a cell can regulate the expression of the protein by reducing the a parameter. When a is above the critical value $a_c = \frac{1}{2b}$, all trajectories flow towards the stable node at the origin, and the protein's expression is suppressed. As a is decreased below a_c, the two other fixed points appear, and the saddlepoint separates initial points whose trajectories flow towards the origin from those that flow towards the fixed point at large protein expression. It can be seen from the figure that when $a < a_c$ the region of the phase portrait for which trajectories flow to the origin is smaller than the region for which they flow to the non-zero stable node, and it shrinks further as a decreases. The saddlepoint therefore acts as a switch separating the two states of suppressed protein expression and high protein expression.

It might be asked what we have gained compared to the 1D model of Chapter 2, given that both models exhibit similar switch-like behaviour. The production of protein in the 1D model

was represented by a constant "source" term, whose value is an arbitrary parameter. In the 2D model, the protein's production is linked to the dynamics of the mRNA. When the parameters a, b satisfy $a < a_c = 1/2b$, a transient increase of mRNA concentration from a low level (or zero) will "flip" the switch above the stable manifold of the saddlepoint, and the protein's expression will increase until the system reaches the stable node with high protein/high mRNA concentrations. Subsequently, if the mRNA concentration is transiently reduced to zero, the system will flow back to the same stable node. So, the model captures the response of protein production to a burst of mRNA, which can only be reversed if the protein is removed by an additional mechanism other than reducing the mRNA concentration. It is therefore a more realistic model of protein production, and contains features that we can imagine extending further.

7.3 Hopf bifurcation in 2D systems

We know from Chapter 3 that trajectories in 2D dynamical systems have more possibilities for their long-time behaviour than monotonically approaching a fixed point or moving off to infinity, which are all that a 1D system can achieve. Oscillatory solutions include spirals, centres, and limit cycles. The previous section demonstrated switch-like behaviour in a 2D system. In this section we look at more complex oscillatory behaviour in which a stable fixed point loses its stability in a bifurcation, a process that can give rise to dangerously unstable dynamics in real systems.

Suppose a 2D system has a stable fixed point (node or spiral) for certain parameter values. In what ways can this fixed point lose stability as the parameters change? By assumption, the eigenvalues of the Jacobian at the fixed point must be both real and negative or complex conjugates with negative real parts. In the former case, if one of the eigenvalues becomes positive, the fixed point undergoes a saddlenode, transcritical, or pitchfork bifurcation. These can be studied using the methods of Chapter TBD. However, if a pair of complex conjugate eigenvalues cross the imaginary axis, so that their real parts become positive, a new form of bifurcation occurs: the Hopf bifurcation. This represents oscillatory behaviour that changes from being stable (i.e., limited in magnitude) to unstable (i.e., potentially growing without bound), and can be dangerous is physical systems.

7.3.1 Supercritical Hopf bifurcation

Consider a 2D system that contains a stable spiral fixed point at the origin; its stability implies that small perturbations die away via damped oscillations. Now suppose that as a parameter is changed, these oscillations do not die away but grow in magnitude and remain stable thereafter. In this case, the stable spiral has changed to an unstable spiral surrounded by a stable limit cycle that pops into existence at a critical parameter value. This type of bifurcation is called a supercritical Hopf bifurcation.

A simple example of this type of bifurcation is the following. We write it in plane polar coordinates (r, θ) for simplicity:

$$\frac{dr}{dt} = \mu r - r^3 \tag{7.24}$$

$$\frac{d\theta}{dt} = \omega + br^2. \tag{7.25}$$

Note the meaning of the three parameters: μ controls the stability of the fixed point at the origin; ω is the frequency of small oscillations near the bifurcation point; and b couples the frequency of the oscillations to their amplitude.

Although it is simpler to visualize the dynamics in plane polar coordinates, we convert to Cartesian coordinates to examine the stability of the fixed point at the origin. Using the substitutions $x = r\cos\theta$ and $y = r\sin\theta$, Equations 7.24 and 7.25 become:

$$\frac{dx}{dt} = \mu x - \omega y - (x + by)(x^2 + y^2), \tag{7.26}$$

$$\frac{dy}{dt} = \omega x + \mu y + (bx - y)(x^2 + y^2). \tag{7.27}$$

The Jacobian is easily found to be:

$$J = \begin{pmatrix} \mu & -\omega \\ \omega & \mu \end{pmatrix}$$

with trace and determinant:

$$\tau = 2\mu \qquad\qquad\qquad\qquad \Delta = \mu^2 + \omega^2.$$

We see that the fixed point is never a saddlepoint because Δ is always greater than zero, and it is stable when $\mu < 0$ and unstable when $\mu > 0$. There is a bifurcation at the critical value $\mu = \mu_c = 0$. One may show that the eigenvalues of the Jacobian are:

$$\lambda = \mu \pm i\omega, \tag{7.28}$$

indicating that the eigenvalues cross the imaginary axis as μ increases through zero.

If we compare the radial Equation 7.24 with that of the supercritical pitchfork bifurcation 7.5 in Section 7.1.3, we see they are identical. The supercritical Hopf bifurcation is the two-dimensional analogue of the supercritical pitchfork bifurcation, with the radial coordinate undergoing a bifurcation and the azimuthal coordinate exhibiting oscillatory behaviour around the fixed point.

When $\mu < 0$, the origin is the only fixed pointin the system, and it is a stable spiral, as may be shown by considering the sign of $\tau^2 - 4\Delta$. But for $\mu > 0$, Equation 7.24 admits two other fixed points : $r^* = \sqrt{\mu}$, and $r^* = -\sqrt{\mu}$. We only consider the positive root because the negative one is meaningless in polar coordinates. Taken together with the azimuthal equation, the new fixed point represents a stable limit cycle whose radius increases from zero as $\sqrt{(\mu)}$ as μ increases. Figure 7.13 shows Graph 1 for the radial equation for values of the parameter μ less than, equal to, and greater than zero.

The fact that the radius of the limit cycle grows continuously with the size of the parameter μ, shows that the change in the dynamics at the bifurcation point is slow, and this gives rise to the other names for this kind of bifurcation. The supercritical Hopf bifurcation is also referred to as "slow", "soft" or a "safe" bifurcation. The meaning of the term safe will become clear when we examine the subcritical Hopf bifurcation in the next section.

What does the bifurcation diagram for this system look like? Unlike in the 1D case, we now need a three-dimensional plot; we draw the parameter μ along one axis, and orient the XY axes orthogonal to this. Figure TBD shows the stable spiral at the origin for $\mu < 0$, and the unstable spiral surrounded by a stable limit cycle of radius $\sqrt{\mu}$ for $\mu > 0$. Notice that all trajectories beginning outside the limit cycle are attracted to it, as is evident from Equation 7.24.

It is important to understand that the Hopf bifurcation is a *local* property of the dynamical equations at the bifurcation point. In the model just discussed, the radius of the limit cycle increases,
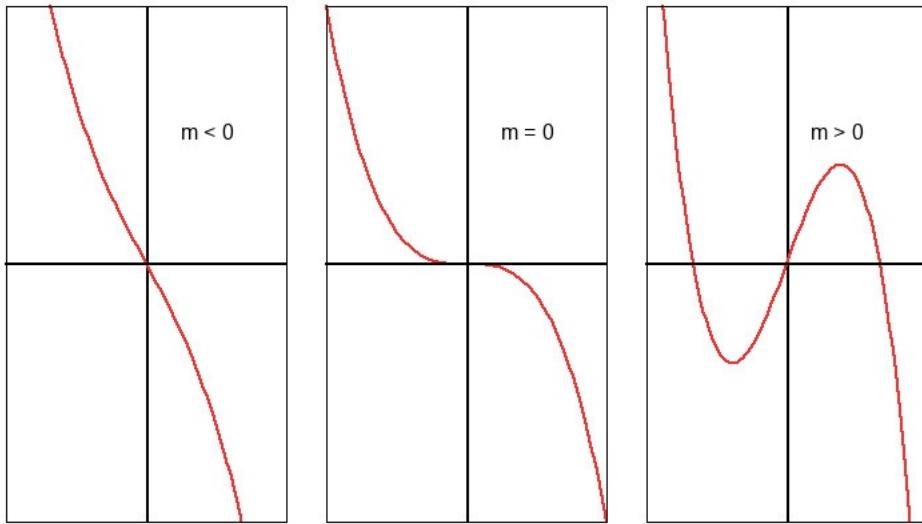
Fig. 7.13. The radial equation dr/dt versus r for the system described by Equations 7.24 and 7.25 for the cases $\mu < 0$, $\mu = 0$, $\mu > 0$ (cp. Figure 7.5) The stable fixed point at the origin becomes unstable as μ passes through zero, and two new stable fixed points appear at $\pm\sqrt{(\mu)}$. But only the positive fixed point makes physical sense in the two-dimensional phase plane.

but no further bifurcations occur, as μ becomes larger. This is not true in general; additional bifurcations may occur at other values of μ, but if they do, they do not affect the existence of the Hopf bifurcation at $\mu = 0$. Clearly, any additional bifurcations require a more complex pair of dynamical equations than Equations 7.24 and 7.25.

7.3.2 Subcritical Hopf bifurcation

Just as the 1D pitchfork bifurcation had two forms — the super and subcritical cases — so has the Hopf bifurcation. The canonical form of the equations for the subcritical Hopf bifurcation are:

$$\frac{dr}{dt} = \mu r + r^3 - r^5 \tag{7.29}$$

$$\frac{d\theta}{dt} = \omega + br^2. \tag{7.30}$$

where the parameters have the same meaning as for the supercritical case in Equations 7.24 and 7.24. The key difference is that the positive r^3 term destabilises the dynamical system, pulling trajectories away to infinity, and this is opposed by the new $-r^5$ term. Note that we add a fifth power instead of a fourth power to retain the symmetry of the equations.

Rewriting these equations in Cartesian coordinates using the same method as in the previous section gives the following dynamical equations:

$$\frac{dx}{dt} = \mu x - \omega y + (x - by)(x^2 + y^2) - x(x^2 + y^2)^2, \tag{7.31}$$

$$\frac{dy}{dt} = \omega x + \mu y + (bx + y)(x^2 + y^2) - y(x^2 + y^2)^2. \tag{7.32}$$
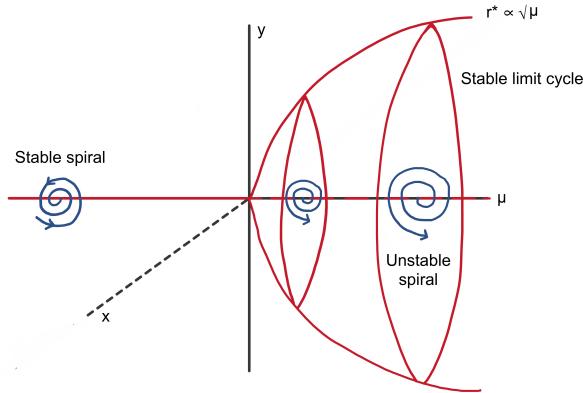
Fig. 7.14. Bifurcation diagram for the supercritical Hopf bifurcation described by Equations 7.24 and 7.25. The stable spiral at the origin becomes unstable as μ increases through zero, and a stable limit cycle appears, whose radius increases continuously as $\sqrt{\mu}$.

The Jacobian for this case can easily be shown to be the same as for the supercritical Hopf bifurcation, namely:

$$J = \begin{pmatrix} \mu & -\omega \\ \omega & \mu \end{pmatrix}$$

with (obviously) the same trace and determinant as before:

$$\tau = 2\mu \qquad\qquad\qquad \Delta = \mu^2 + \omega^2.$$

This shows that a linearisation of the dynamical equations does not distinguish between the super and subcritical cases. One has to examine the non-linear terms in order to identify the type of the fixed point correctly. From the Jacobian ,we find again that the fixed point at the origin for $\mu < 0$ is a stable spiral that becomes unstable for $\mu > 0$.

In order to find the location of the non-zero fixed point(s) when $\mu > 0$ we need to find solutions of the radial equation 7.29. This may be rewritten in the form:

$$\frac{dr}{dt} = -r(r^2 - r_-^2)(r^2 - r_+^2) \tag{7.33}$$

where the roots are given by:

$$r_\pm^2 = \frac{1 \pm \sqrt{1 + 4\mu}}{2}. \tag{7.34}$$

Figure 7.15 shows Graph 1 for the radial coordinate of the subcritical Hopf bifurcation model for a sequence of values of parameter μ.

We next examine the various regimes of the solution as the parameter μ is increased from an initially-negative value.

Case 1 $\mu < -\frac{1}{4}$

In this case, the two roots in Equation 7.34 are complex, so the origin is the only fixed point, and it is a stable spiral.
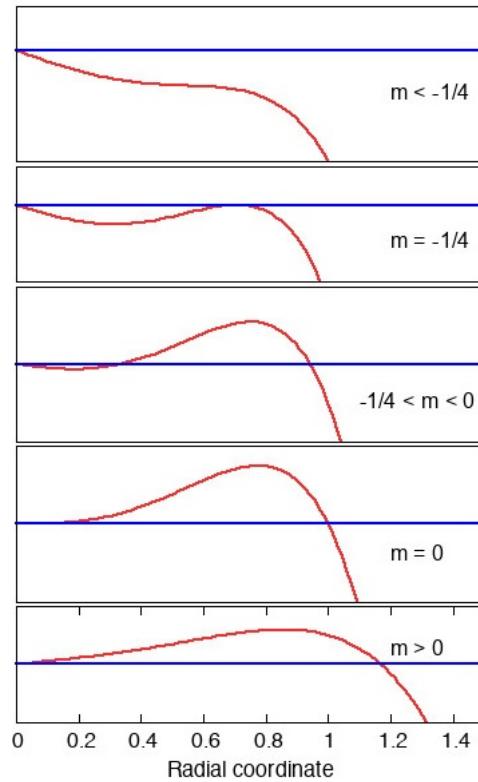
Fig. 7.15. The radial component of the vector field for a 2D dynamical system undergoing a subcritical Hopf bifurcation described by Equations 7.29 and 7.30. The graphs correspond to the five cases in the text as the control parameter increases in value. The stable spiral at the origin becomes unstable as μ passes through zero, and an unstable and a stable limit cycle appear at radial coordinates that are not proportional to μ, but take on values of O(1).

Case 2 $\mu = -\frac{1}{4}$

The two roots coalesce into one here $r = \frac{1}{\sqrt{(2)}}$. A key point to note here is that the magnitude of the radial coordinate of this solution does not depend on the value of the parameter μ, which has vanished from Equation 7.34. Hence, the limit cycle that appears for any $\mu > -\frac{1}{4}$ occurs at a potentially large distance away from the origin.

Case 3 $-\frac{1}{4} < \mu < 0$

The two roots are distinct here and given by the above Equation 7.34. The $r-$ solution represents an unstable limit cycle that circles around the stable spiral at the origin, while the $r+$ solution is a stable limit cycle farther out. All trajectories originating beyond the stable limit cycle are attracted to it, as are those that being between the unstable and stable limit cycle. As μ is increased towards zero, the unstable limit cycle shrinks to encompass the spiral at the origin, and changes it to an unstable spiral.

Case 4 $\mu = 0$

The two roots are now $r_- = 0$ and $r_+ = 1$, and are an unstable spiral at the origin and stable limit cycle respectively. Note again that the radius of the stable spiral is O(1), and not proportional to the magnitude of the parameter μ. This is the origin of the labels "discontinuous" and "dangerous" for

the subcritical Hopf bifurcation: once the transition point is passed, trajectories are drawn towards the only stable fixed point left in the system, which is the limit cycle at a large distance from the previously stable spiral at the origin.

Case 5 $\mu > 0$

For all values of μ greater than zero, the negative root is complex, leaving only the positive root $r_+^2 = \frac{1+\sqrt{1+4\mu}}{2}$ as the only solution, and it remains a stable limit cycle whose radius continuous to increase as μ increases.

The bifurcation diagram for the subcritical Hopf bifurcation is shown in Figure 7.16. By comparison with Figure 7.9, it can be seen that the behaviour of the radial coordinage in a subcritical Hopf bifurcation is essentially the same as the one-dimensional subcritical pitchfork bifurcation. The motion of the system in two dimensions is oscillatory around the given radial fixed point. There are two important points to note: as the parameter μ is increased above zero, the system jumps from the stable spiral at the origin to the possibly very distant stable limit cycle. It is the fact that the stable branch can be arbitrarily far from the origin that makes the subcritical Hopf bifurcation dangerous in practical situations, because it implies that oscillations that were damped below the bifurcation point will become arbitrarily large above it. Second, once the system is on the (distant) stable limit cycle branch, it can only be returned to the stable spiral (at the origin) after a larger reduction of μ to below $-\frac{1}{4}$. This has the practical consequence that a system that has passed through a subcritical Hopf bifurcation will continue to exhibit potentially dangerous large oscillations until the control parameter is reduced below the value at which the oscillations began.
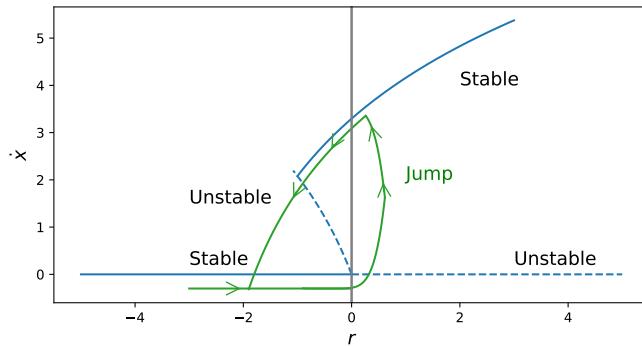

Fig. 7.16. Bifurcation diagram for a dynamical system undergoing a subcritical Hopf bifurcation, as a function of the control parameter μ. Note the similarity of this diagram with that of the subcritical pitchfork diagram in Fig. 7.9. The stable spiral that exists at the origin when $\mu < -1/4$ becomes unstable at $\mu = 0$, and the system jumps to the stable limit cycle that already appeared at $\mu < -1/4$ but to which it was unable to move because of the unstable limit cycle in between. On reducing μ, the system will not return to the original stable limit cycle until $\mu < -1/4$. The system therefore exhibits hysteresis.